Title

14-3-3-zeta mediates GLP-1 receptor agonist action to alter α cell proglucagon processing.

Journal

Science Advances, 8(29)

Authors

Holter, Marlena
Phuong, Daryl
Lee, Isaac
et al.

Publication Date

2022-07-22

DOI

10.1126/sciadv.abn3773

Peer reviewed

HEALTH AND MEDICINE

14-3-3-zeta mediates GLP-1 receptor agonist action to alter α cell proglucagon processing

Marlena M. Holter[1], Daryl J. Phuong[1], Isaac Lee[1], Mridusmita Saikia[1,2], Lisa Weikert[1], Samantha Fountain[1], Elizabeth T. Anderson[3], Qin Fu[3], Sheng Zhang[3], Kyle W. Sloop[4], Bethany P. Cummings[1,5]*

Recent studies demonstrate that α cells contribute to glucose-stimulated insulin secretion (GSIS). Glucagon-like peptide-1 receptor (GLP-1R) agonists potently potentiate GSIS, making these drugs useful for diabetes treatment. However, the role of α and β cell paracrine interactions in the effects of GLP-1R agonists is undefined. We previously found that increased β cell GLP-1R signaling activates α cell GLP-1 expression. Here, we characterized the bidirectional paracrine cross-talk by which α and β cells communicate to mediate the effects of the GLP-1R agonist, liraglutide. We find that the effect of liraglutide to enhance GSIS is blunted by α cell ablation in male mice. Furthermore, the effect of β cell GLP-1R signaling to activate α cell GLP-1 is mediated by a secreted protein factor that is regulated by the signaling protein, 14-3-3-zeta, in mouse and human islets. These data refine our understanding of GLP-1 pharmacology and identify 14-3-3-zeta as a potential target to enhance α cell GLP-1 production.

INTRODUCTION

The pancreatic islet α and β cells are traditionally described as working in opposition to one another, with β cells producing insulin to lower blood glucose and α cells producing glucagon to increase hepatic glucose production. However, recent studies have established that α cells contribute to glucose-stimulated insulin secretion (GSIS), suggesting that their role in glucose regulation and islet function is more complex than previously appreciated. Glucagon-like peptide-1 receptor (GLP-1R) agonists have become increasingly popular for the treatment of type 2 diabetes mellitus, in part, because of their potent incretin effect to enhance GSIS from β cells. The model by which endogenously produced GLP-1 was thought to contribute to the incretin effect has been revisited in recent years. This model postulates that GLP-1 secretion from gut enteroendocrine L cells acts via the circulation on the β cell GLP-1R to enhance GSIS in response to a meal (*1*, *2*). However, the minimal postprandial increases in circulating active GLP-1 and the short half-life of active GLP-1 point to inconsistencies between circulating GLP-1 levels and β cell GLP-1R function (*3*, *4*). These shortcomings have motivated the field to intensively revisit the mechanisms governing the incretin effect of GLP-1. Progress has been made in revising our understanding of the physiology of endogenously produced GLP-1. However, how these conceptual changes in our understanding of endogenous GLP-1 biology may affect our understanding of the mechanisms by which GLP-1R agonists regulate islet function is incompletely understood.

GLP-1, shares the same precursor protein as glucagon, proglucagon. Canonically, it was thought that proglucagon is differentially processed depending on where it is expressed. The tissue-specific processing of proglucagon was thought to be due to the tissue-specific expression of the processing enzymes, prohormone convertase 1/3 (protein: PC1/3, gene: *Pcsk1*) and prohormone convertase 2 (protein: PC2, gene: *Pcsk2*). PC1/3 activity in L cells produces GLP-1, and PC2 activity in α cells yields glucagon. It was previously thought that α cells only express PC2 and thus can only process proglucagon into glucagon. However, in recent years, a growing body of literature has reported that under physiological conditions (postnatal development) and pathophysiological conditions (type 1 and 2 diabetes mellitus), α cells can express PC1/3, enabling production of active GLP-1 (*5*–*15*). Thus, it is possible to shift α cell proglucagon processing from glucagon to GLP-1 to enhance GSIS and reduce hepatic glucagon action. In line with this, several studies have found that pancreatic proglucagon-derived peptides may be more important than gut-derived proglucagon products in glycemic control (*16*, *17*). Furthermore, recent studies have shown that α cells contribute to insulin secretion (*16*, *18*–*20*). However, the role of α cells in the β cell GLP-1R–mediated effects of GLP-1R agonists is incompletely defined.

We previously reported that surgically and pharmacologically enhanced β cell GLP-1R signaling activates α cell PC1/3 and GLP-1 expression in mice (*21*, *22*). Similarly, treatment of human islets with a GLP-1R agonist increases α cell *PCSK1* expression and islet-active GLP-1 production (*21*). However, the role of the α cell in the glucoregulatory effects of GLP-1R agonist treatment and the mechanisms by which GLP-1R agonist treatment activates α cell GLP-1 production are unknown. Therefore, we tested the hypothesis that the effects of GLP-1R agonist treatment to improve GSIS are dependent, at least in part, on α cells. Furthermore, we tested the hypothesis that enhanced β cell GLP-1R signaling activates α cell GLP-1 production through paracrine signaling factors. We find that the effect of GLP-1R agonist treatment to enhance insulin secretion is blunted by α cell ablation in male, but not female, mice. Furthermore, we find that the effect of enhanced β cell GLP-1R signaling to induce α cell GLP-1 production is dependent on a secreted protein factor. Last, using untargeted proteomics and in vitro functional validation, we identify the signaling protein, 14-3-3-zeta, as a mediator of the effect of GLP-1R agonist treatment to activate α cell GLP-1 production. Together, our results underscore the importance of bidirectional cross-talk between α and β cells in GLP-1 pharmacology and point

[1]Department of Biomedical Sciences, Cornell University, College of Veterinary Medicine, Ithaca, NY, USA. [2]Nancy E. and Peter C. Meinig School of Biomedical Engineering, Ithaca, NY, USA. [3]Proteomics and Metabolomics Facility, Institute of Biotechnology, Cornell University, Ithaca, NY, USA. [4]Diabetes and Complications, Lilly Research Laboratories, Eli Lilly and Company, Indianapolis, IN, USA. [5]Department of Surgery, Center for Alimentary and Metabolic Sciences, School of Medicine, University of California, Davis, Sacramento, CA, USA.
*Corresponding author. Email: bpcummings@ucdavis.edu

to 14-3-3-zeta as a potential target with which to enhance α cell GLP-1 production for diabetes treatment.

RESULTS

β Cell GLP-1R knockout and α cell ablation impairs liraglutide-induced activation of islet GLP-1 production and improvements in islet function

We previously reported that the GLP-1R agonist, liraglutide, activates islet GLP-1 expression in a β cell GLP-1R–dependent fashion in high-fat diet (HFD)–fed mice (*21*). However, the role of the α cell in the metabolic benefits of liraglutide is unknown. To determine the role of the β cell GLP-1R and the α cell in the metabolic effects of liraglutide treatment, male and female HFD-fed tamoxifen-inducible β cell–specific GLP-1R wild-type (WT) and knockout (KO) mice (*23*, *24*) along with β cell GLP-1R WT mice with diphtheria toxin (DT)–inducible α cell ablation (*25*) were studied. Mice were fed HFD to induce obesity and metabolic stress so that liraglutide treatment was studied under a translationally relevant condition. Furthermore, the study was designed to match the experimental conditions previously validated to induce α cell GLP-1 expression in this mouse model (*21*). Mice were placed on a 60% energy-from-fat HFD starting at 8 weeks of age and continuing throughout the duration of study. After 8 to 10 weeks of HFD feeding, all mice were placed on HFD supplemented with tamoxifen throughout the rest of study to induce β cell GLP-1R KO, and all mice received DT (500 ng of DT per intraperitoneal injection, given once every other day for three doses) to induce α cell ablation, as previously validated (*20*). All mice received tamoxifen and DT such that these variables did not differ between groups and thus were not confounders. Two weeks after the start of tamoxifen and DT administration, male and female *GcgDTR*$^{-}$*-Glp-1r*$^{\beta\ cell+/+}$ [*MIPCreERT*$^{-}$*-hGlp-1r*] [WT DTR^{-} (diphtheria toxin receptor)] and *GcgDTR*$^{-}$*-Glp-1r*$^{\beta\ cell-/-}$ [*MIPCreERT*$^{+}$*-hGlp-1r*] (KO DTR^{-}) littermates and *GcgDTR*$^{+}$*-Glp-1r*$^{\beta\ cell+/+}$ [*MIPCreERT*$^{-}$*-hGlp-1r-GcgDTR*$^{+}$] (WT DTR^{+}) littermates were given twice daily injections (200 μg/kg of body weight subcutaneously) of liraglutide or an equal volume of saline. Mice underwent an oral glucose tolerance test (OGTT) after 2 weeks and an intraperitoneal glucose tolerance test (IPGTT) after 3 weeks of liraglutide or saline treatment to assess the contribution of α cells and the β cell GLP-1R to the metabolic effects of liraglutide with and without gut-derived GLP-1. These GTT time points were chosen on the basis of our previous work validating that 2 weeks of liraglutide treatment in this study paradigm activates α cell GLP-1 expression (*21*). Mice were euthanized for tissue collection following the IPGTT. Body weight did not differ between groups, enabling the assessment of glucose tolerance independently of body weight (fig. S1, A and E). Liraglutide decreased white adipose tissue weight compared to controls in the β cell GLP-1R WT mice with functional α cells, and liraglutide decreased brown adipose tissue depot weight compared to controls in the β cell GLP-1R WT mice with α cell ablation (fig. S1; $P \leq 0.05$).

Consistent with prior work in the *GcgDTR* mouse model (*25*), *DTR*$^{+}$ mice exhibited almost complete loss of α cells (less than 2% of α cells remaining) (Fig. 1, A and B; $P < 0.0001$). This was accompanied by a significant reduction in fasting serum glucagon concentrations (Fig. 1C; $P < 0.01$). The lack of a complete loss of circulating glucagon in the face of DTR-induced α cell ablation has been previously observed in this mouse model and demonstrated to not be a product of increased extrapancreatic glucagon production and, instead, was suggested to be due to glucagon secretion from the few remaining α cells (*25*). Similar to our previous work (*21*), liraglutide treatment increased islet GLP-1 expression in a β cell GLP-1R–dependent manner (Fig. 1, A and D; $P < 0.0001$). Liraglutide did not induce islet GLP-1 expression in mice with α cell ablation, suggesting that α cells are the cell type of origin for GLP-1–expressing islet cells.

In mice with functional α cells, liraglutide treatment improved oral glucose tolerance compared to saline-treated controls in both β cell GLP-1R WT and KO mice (Fig. 2, A and B; $P < 0.01$). However, glucose excursions were higher in β cell GLP-1R KO mice compared with WT under both saline- and liraglutide-treated conditions (Fig. 2, A and B; $P < 0.05$). The effect of liraglutide to improve glucose regulation in β cell GLP-1R KO mice may be due to extrapancreatic effects of liraglutide, such as a reduction in gastric emptying (*26*, *27*). Consistent with the glycemic effects, liraglutide increased insulin secretion in β cell GLP-1R WT, but not in β cell GLP-1R KO mice, during the OGTT (Fig. 2C; $P < 0.0001$).

During the IPGTT, a condition in which circulating levels of gut-derived hormones should remain unchanged from baseline, liraglutide treatment improved glucose tolerance compared to saline-treated controls in β cell GLP-1R WT mice but not in KO mice (Fig. 2, D and E; $P < 0.001$). Intraperitoneal glucose tolerance did not differ between saline-treated β cell GLP-1R WT and KO mice (Fig. 2, D and E). Similar to the OGTT, liraglutide increased insulin secretion in β cell GLP-1R WT but not in β cell GLP-1R KO mice, during the IPGTT (Fig. 2F; $P < 0.05$). Overall, these findings demonstrate that the β cell GLP-1R contributes to liraglutide-mediated improvements glucose tolerance and GSIS in HFD-fed mice. To control for the presence of MIP-CreERT, we studied *Cre*$^{-}$ and *Cre*$^{+}$ littermates homozygous for the floxed GLP-1R allele (*MIPCreERT-hGlp-1r*) without tamoxifen administration. There was no difference in glucose tolerance between Cre^{+} and Cre^{-} mice during an OGTT or IPGTT in the absence of tamoxifen, which suggests that MIPCreERT was not a confounding factor (fig. S2).

To determine the contribution of α cells to the metabolic effects of liraglutide, we examined the effect of liraglutide on glucose tolerance and insulin secretion in mice with α cell ablation. OGTT and IPGTT data from mice with α cell ablation (WT DTR^{+}) are presented with data from β cell GLP-1R WT mice without α cell ablation (WT DTR^{-}, also presented in Fig. 2) to facilitate comparison. During the OGTT, liraglutide improved glucose tolerance and insulin secretion to a similar degree in mice with and without α cell ablation (fig. S3, A to C; $P < 0.01$). These data suggest that in the presence of gut-derived hormones, paracrine signaling interactions between α and β cells are not necessary for the glucoregulatory benefits of liraglutide. Similarly, during the IPGTT, liraglutide improved glucose tolerance and insulin secretion to a similar degree in mice with and without α cell ablation (fig. S3, D to F; $P < 0.05$). However, when analyzed separately by sex, while there was a trend for liraglutide to improve glucose tolerance in male mice with α cell ablation, this did not reach significance (Fig. 3, A and B). This was paralleled by impaired insulin secretion in response to liraglutide in male mice with α cell ablation (Fig. 3C). These findings suggest that metabolic responses to α cell ablation are regulated in a sex-specific manner. Further work is needed to understand the impact of sex on paracrine interactions between α and β cells. Together, these data suggest that in the absence of gut-derived GLP-1, paracrine signaling interactions between α and β cells contribute liraglutide-mediated enhancements in β cell insulin secretory function in male mice.

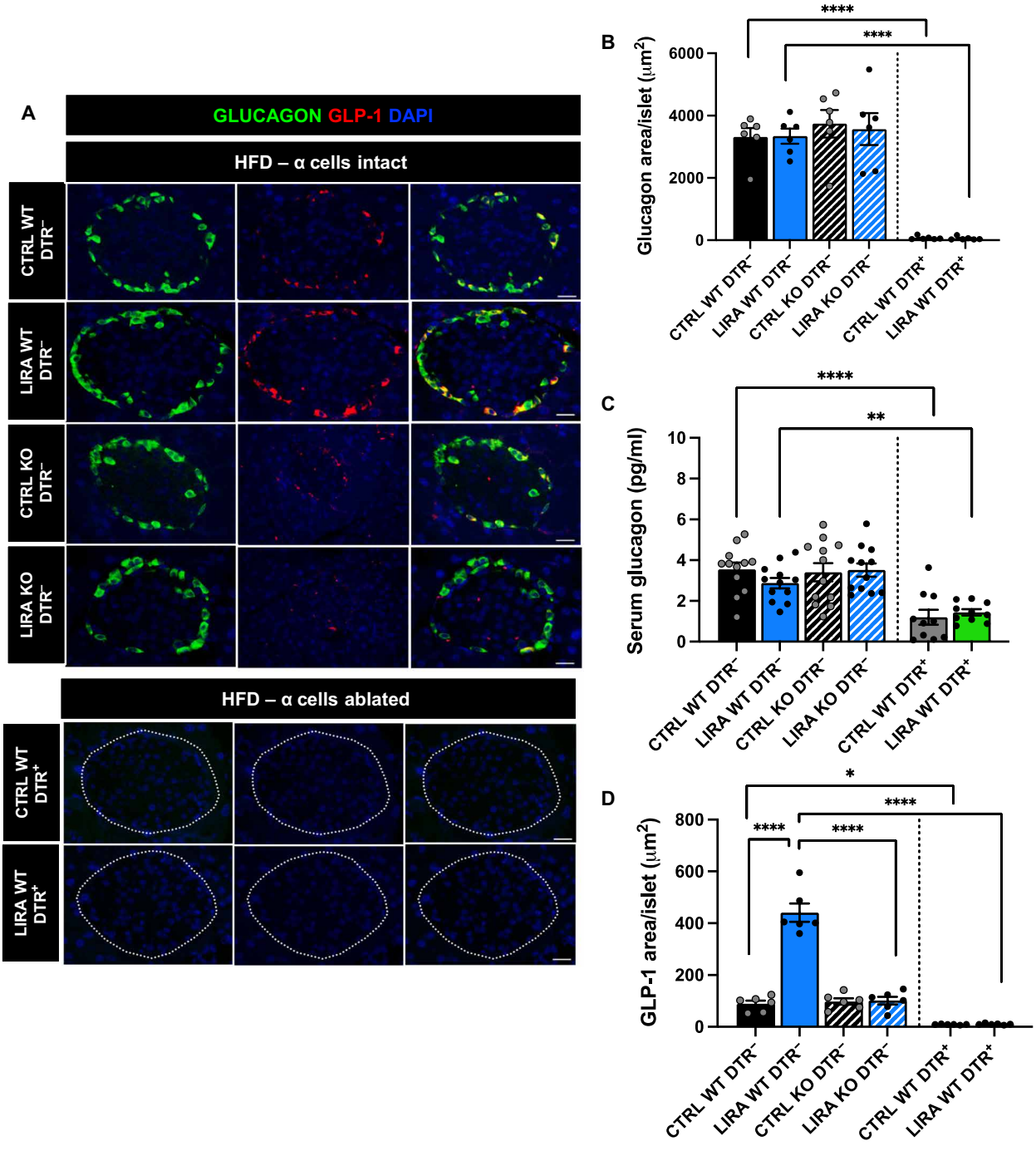

Fig. 1. Liraglutide increases islet GLP-1 expression in a β cell GLP-1R–dependent and α cell–dependent manner. (**A**) Representative images of mouse pancreas sections immunostained for glucagon (green), GLP-1 (red), and 4′,6′-diamidino-2-phenylindole (DAPI) in saline (CTRL) and liraglutide (LIRA)–treated male and female *GcgDTR*$^{-}$*-Glp-1r*$^{\beta\,cell+/+}$ [*MIPCreERT*$^{-}$*-hGlp-1r*] (WT DTR^{-}) and *GcgDTR*$^{-}$*-Glp-1r*$^{\beta\,cell-/-}$ [*MIPCreERT*$^{+}$*-hGlp-1r*] (KO DTR^{-}) littermates and *GcgDTR*$^{+}$*-Glp-1r*$^{\beta\,cell+/+}$ [*MIPCreERT*$^{-}$*-hGlp-1r* with *GcgDTR*$^{+}$] (WT DTR^{+}) littermates. (**B**) Average glucagon staining per islet in β cell GLP-1R WT DTR^{-} and KO DTR^{-} mice and in β cell GLP-1R WT DTR^{+} mice following 3 weeks of liraglutide treatment. (**C**) Fasting serum glucagon concentrations in β cell GLP-1R WT DTR^{-} and KO DTR^{-} mice and in β cell GLP-1R WT DTR^{+} mice following 2 weeks of saline or liraglutide treatment. (**D**) Average GLP-1 staining per islet in β cell GLP-1R WT DTR^{-} and KO DTR^{-} mice and in β cell GLP-1R WT DTR^{+} mice following 3 weeks of saline or liraglutide treatment. Data are presented as means ± SEM. $n = 6$ to 12 per group. *$P < 0.05$, **$P < 0.01$, ****$P < 0.0001$ by two-factor analysis of variance (ANOVA) with Bonferroni's posttest. Scale bar, 20 μm.

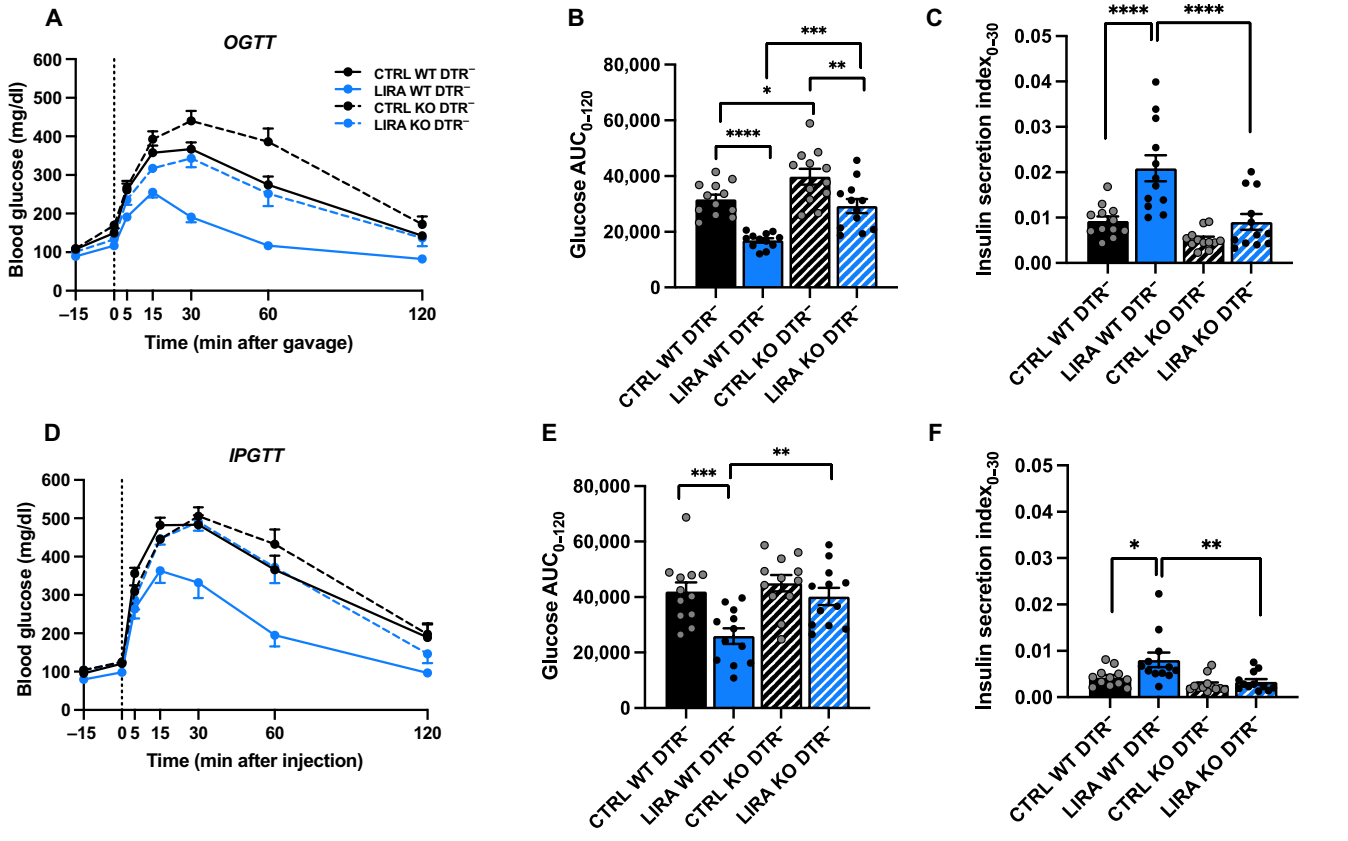

Fig. 2. β Cell GLP-1R KO impairs liraglutide-induced improvements in glucose tolerance. (**A**) Blood glucose concentrations, (**B**) glucose area under the curve (AUC), and (**C**) insulin secretion index during an OGTT in male and female *GcgDTR*$^{-}$*-Glp-1r*$^{\beta\ cell+/+}$ [*MIPCreERT*$^{-}$*-hGlp-1r*] (WT DTR^{-}) and *GcgDTR*$^{-}$*-Glp-1r*$^{\beta\ cell-/-}$ [*MIPCreERT*$^{+}$*-hGlp-1r*] (KO DTR^{-}) mice with functional α cells following 2 weeks of saline (CTRL) or liraglutide (LIRA) treatment. (**D**) Blood glucose concentrations, (**E**) glucose AUC, and (**F**) insulin secretion index during an IPGTT in β cell GLP-1R WT and KO mice following 3 weeks of saline or liraglutide treatment. In all conditions, liraglutide or saline was administered 15 min before glucose administration. Data are presented as means ± SEM. $n = 12$ per group. *$P < 0.05$, **$P < 0.01$, ***$P < 0.001$, ****$P < 0.0001$ by two-factor ANOVA with Bonferroni's posttest.

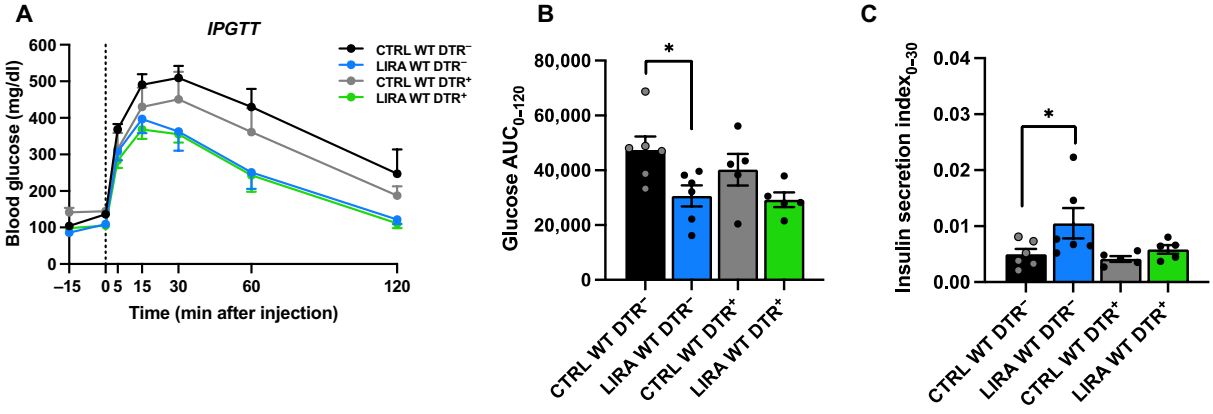

Fig. 3. α Cell ablation impairs liraglutide-induced insulin secretion in response to intraperitoneal glucose challenge in male mice. (**A**) Blood glucose concentrations, (**B**) glucose AUC, and (**C**) insulin secretion index during an IPGTT in male *GcgDTR*$^{-}$*-Glp-1r*$^{\beta\ cell+/+}$ [*MIPCreERT*$^{-}$*-hGlp-1r*] (WT DTR^{-}) littermates with α cells and *GcgDTR*$^{+}$*-Glp-1r*$^{\beta\ cell+/+}$ [*MIPCreERT*$^{-}$*-hGlp-1r* with *GcgDTR*$^{+}$] (WT DTR^{+}) littermates without α cells following 3 weeks of saline (CTRL) or liraglutide (LIRA) treatment. In all conditions, liraglutide or saline was administered 15 min before glucose administration. Data are presented as means ± SEM. $n = 5$ to 6 per group. *$P < 0.05$ by two-factor ANOVA with Bonferroni's posttest. Note: Data from male mice in the DTR^{-} groups are also included in the data from the male WT DTR^{-} mice in Fig. 2, D to F.

Pharmacologically enhanced β cell GLP-1R signaling activates α cell GLP-1 production and secretion through a secreted protein

We next sought to determine how β cell GLP-1R signaling activates α cell GLP-1 production. We hypothesized that β cell GLP-1R signaling causes secretion of a factor that acts in a paracrine manner to increase α cell PC1/3 expression. To test this, conditioned media was generated from HFD-fed β cell GLP-1R WT and KO islets isolated from mice studied similarly to the mice described above. Specifically, male and female tamoxifen-inducible *Glp-1r*$^{\beta\,cell+/+}$ (WT) and *Glp-1r*$^{\beta\,cell-/-}$ (KO) littermates received HFD starting at 8 to 11 weeks of age and continuing throughout the duration of study. All mice received tamoxifen such that this was not a variable between groups. Starting after 8 to 10 weeks of HFD feeding, mice received saline or liraglutide injections for 2 weeks, and then islets were isolated for study. Following isolation, islets were stimulated with 11.1 mM glucose + 100 nM of liraglutide or saline for 15 min, and then conditioned media was collected (Fig. 4A). Islets were stimulated with liraglutide in vitro to control for the possibility that the response to in vivo treatment is blunted during islet isolation. Islet numbers per well were consistent between groups and treatments. We focused on the 15-min time point for the generation of conditioned media based on previous work reporting maximal GSIS in response to GLP-1R agonists after 15 min both in vitro (*28*) and in vivo (*29*–*31*). Before experimentation with mouse islets, α TC1 clone 6 (α TC1-6) cells were incubated in saline and liraglutide for 24 hours in the absence of islet-conditioned media to confirm that liraglutide alone does not induce α cell *Pcsk1* expression (Fig. 4B).

To first validate β cell GLP-1R KO, we measured insulin secretion in the conditioned media generated from β cell GLP-1R WT and KO islets used to generate conditioned media for study. Liraglutide treatment enhanced GSIS in both β cell GLP-1R WT and KO islets (Fig. 4C; $P < 0.05$). Consistent with our previous work (*32*), insulin secretion was markedly lower in response to liraglutide treatment in β cell GLP-1R KO compared with β cell GLP-1R WT islets (Fig. 4C; $P < 0.0001$), demonstrating effective β cell GLP-1R KO. GSIS was also lower in saline-treated β cell GLP-1R KO islets compared with saline-treated β cell GLP-1R WT islets, suggesting that β cell GLP-1R signaling contributes to β cell tone and GSIS in the absence of exogenous GLP-1. It is also possible that given that the GLP-1R serves as a marker of β cell maturity (*33*), knockdown of the β cell GLP-1R may result in altered insulin secretory dynamics as a function of β cell immaturity.

To determine whether β cell GLP-1R signaling increases α cell PC1/3 expression through a secreted factor, we applied conditioned media generated from these islets to α TC1-6 α cells for 24 hours (Fig. 4A). Conditioned media from liraglutide-treated islets exposed to liraglutide in culture for 15 min increased α cell *Pcsk1* mRNA expression only if β cells expressed the GLP-1R ($P < 0.01$; Fig. 4D), demonstrating that enhanced β cell GLP-1R signaling activates α cell *Pcsk1* expression through a secreted factor. In addition, the absence of an effect of conditioned media from liraglutide-treated β cell GLP-1R KO islets on α cell *Pcsk1* mRNA expression further demonstrates that liraglutide treatment alone does not induce α cell *Pcsk1* mRNA expression. However, conditioned media generated from islets of liraglutide-treated mice exposed to liraglutide in culture for 2 hours did not alter α cell *Pcsk1* mRNA expression (Fig. 4E), suggesting that the intra-islet–secreted factor(s) is only present in the conditioned media for finite amounts of time.

We then pursued a series of experiments in which the conditioned media was manipulated before treatment of α cells were then pursued to define key characteristics of the paracrine factor. To simplify the study design and test the paracrine system in a different mouse line, we studied WT mice. Mice were studied using the same experimental conditions as the conditioned media study in the β cell GLP-1R WT and KO mice described above to maintain consistency across studies. Similar to the results from the β cell GLP-1R WT and KO mice, conditioned media generated from liraglutide-treated islets increased α cell *Pcsk1* mRNA expression and increased α cell active GLP-1 production compared to conditioned media from saline-treated islets ($P < 0.01$; Fig. 4, F and G). However, this effect was lost in response to conditioned media generated following 2-hour in vitro exposure to liraglutide (Fig. 4F).

To assess whether the intra-islet–secreted factor is a protein, we subjected the conditioned media generated from islets treated with liraglutide or saline for 15 min to either a freeze-thaw cycle or treatment with proteinase K (PK). Both the freeze-thaw cycle and PK treatment ablated the effect of conditioned media from liraglutide-treated islets to increase α cell *Pcsk1* mRNA expression (Fig. 4F). To further characterize the paracrine factor, we fractionated the conditioned media on the basis of molecular weight. The effect of conditioned media from liraglutide-treated islets to increase α cell *Pcsk1* mRNA expression was preserved in the >50-kDa fraction and lost in the <50-kDa fraction ($P < 0.01$; Fig. 4F). This experiment was repeated in β cell GLP-1R WT and KO islets and confirmed that >50-kDa conditioned media from liraglutide-treated islets increased α cell *Pcsk1* mRNA expression in a β cell GLP-1R–dependent manner ($P < 0.01$; Fig. 4H).

To determine whether induction of α cell *Pcsk1* expression results in active GLP-1 secretion, we treated α cells with conditioned media and passed through a centrifugal filter column with a molecular weight cutoff of 50 kDa before treatment. This filtration column enabled removal of low–molecular weight proteins, such as liraglutide, and islet-derived proglucagon and insulin products, such that active GLP-1 concentrations detected in the α cell conditioned media were α cell specific. Consistent with the effect of column-treated conditioned media from liraglutide-treated islets to increase α cell *Pcsk1* expression, this same conditioned media increased α cell secretion of active GLP-1 in a β cell GLP-1R–dependent manner ($P < 0.05$; Fig. 4I). Together, these data demonstrate that β cell GLP-1R signaling activates α cell *Pcsk1* expression and active GLP-1 secretion through a secreted paracrine factor that is a protein retained in the >50-kDa molecular weight fraction.

Decreased 14-3-3-zeta mediates the effect of islet GLP-1R signaling to increase α cell PC1/3 expression and active GLP-1 secretion

To define the paracrine protein factor(s) responsible for the effect of β cell GLP-1R signaling to increase α cell GLP-1 production, we performed label-free quantitative proteomics on conditioned media from islets isolated from β cell GLP-1R WT mice studied, similar to the study designs described above. To narrow down the list of possible candidates, we used only the >50-kDa fraction for proteomics analyses (Fig. 5A). A total of 191 unique proteins were identified. All identified proteins were screened for the presence of a secretion signal by the program SignalP 5.0 (*34*) or identified as a secreted protein through literature search, revealing that 67 of these proteins are predicted to be secreted proteins (Fig. 5B). Orthogonal projections

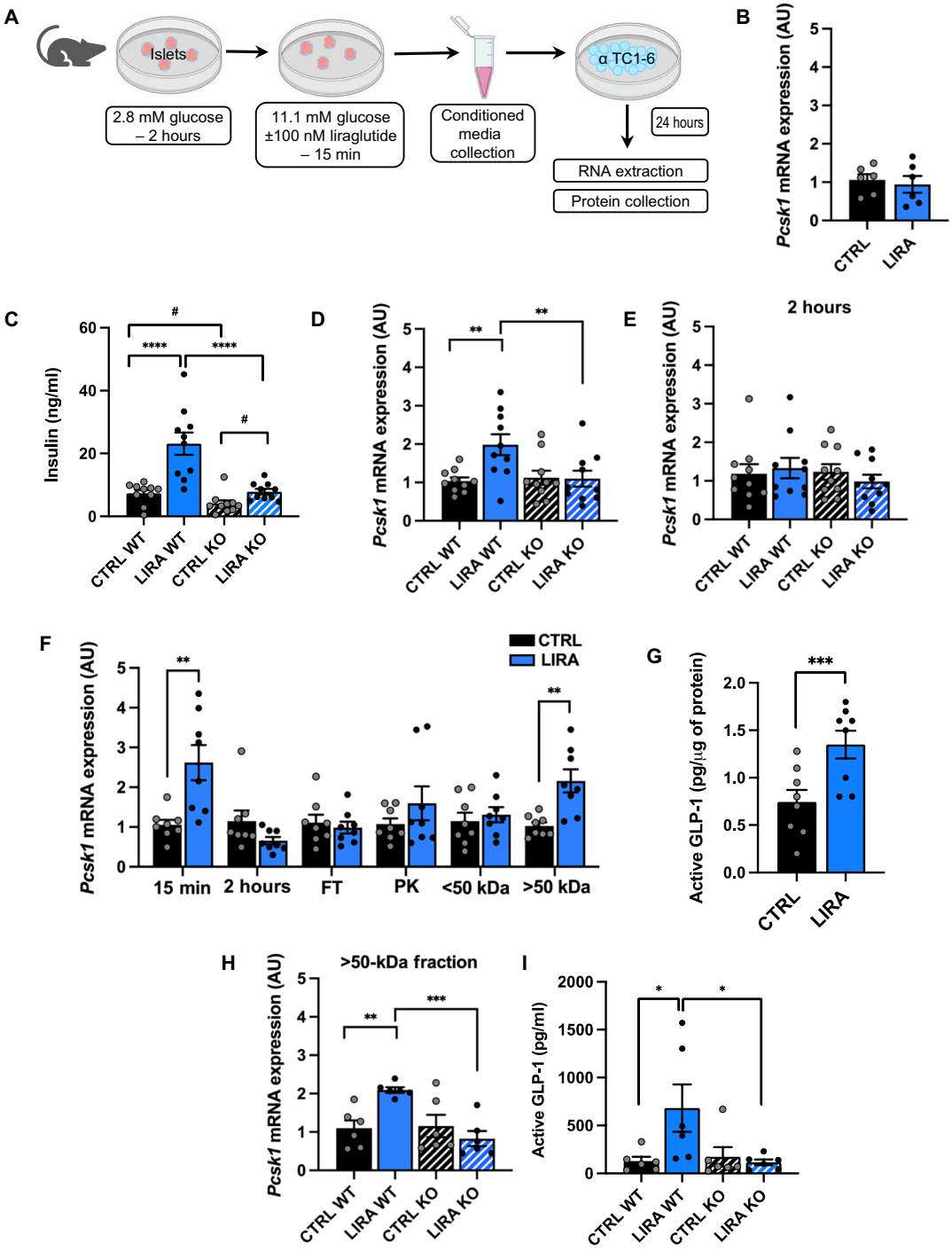

Fig. 4. Pharmacologically enhanced β cell GLP-1R signaling activates α cell GLP-1 production and secretion through a secreted protein factor. (**A**) Schematic of the in vitro study design. (**B**) α Cell *Pcsk1* mRNA expression following treatment with saline or 100 nM liraglutide. (**C**) Insulin secretion from islets isolated from β cell GLP-1R WT and KO mice in response to 11.1 mM glucose with or without 100 nM liraglutide. α Cell *Pcsk1* mRNA expression following treatment with conditioned media generated from islets of saline- (CTRL) and liraglutide (LIRA)–treated β cell GLP-1R WT and KO mice after 15 min (**D**) and 2 hours (**E**) of incubation with saline or liraglutide. (**F**) α Cell *Pcsk1* mRNA expression following treatment with conditioned media generated from islets of saline- and liraglutide-treated WT mice following 15 min and 2 hours of incubation with saline or liraglutide and following treatment with conditioned media samples from the 15-min incubation that were subjected to a freeze-thaw cycle (FT), PK, or fractionated on the basis of molecular weight before application to α cells. (**G**) Active GLP-1 concentrations measured in lysates of α cells treated with conditioned media from the 15-min time point from Fig. 4F. (**H**) α Cell *Pcsk1* mRNA expression and (**I**) active GLP-1 secretion following treatment with conditioned media from the >50-kDa molecular weight fraction generated from islets of β cell GLP-1R WT and KO mice treated with liraglutide or saline for 15 min. Data are presented as means ± SEM. $n = 6$ to 10 per group. $^{*}P < 0.05$, $^{**}P < 0.01$, $^{***}P < 0.001$, $^{****}P < 0.0001$ by two-factor ANOVA with Bonferroni's posttest; $\#P < 0.05$ by Student's t test. AU, arbitrary units.

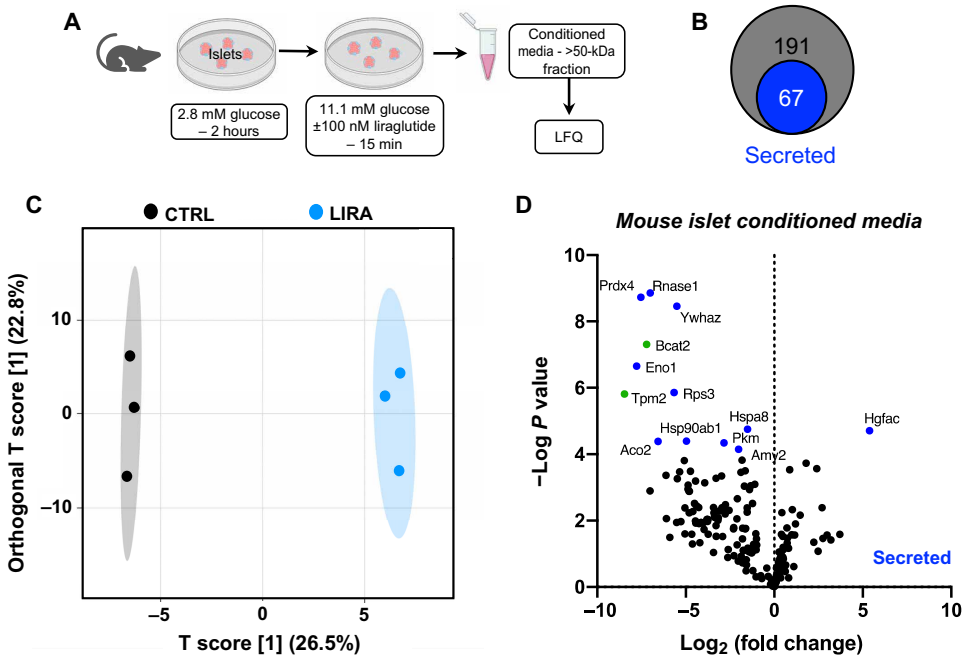

Fig. 5. Impact of liraglutide treatment on islet protein secretion. (**A**) In vitro study paradigm for generation of conditioned media samples used for proteomics analysis. Conditioned media generated from islets of liraglutide- (LIRA) and saline-treated (CTRL) β cell GLP-1R WT mice were digested, and protein signatures were determined using mass spectrometry–based quantitative proteomics. LFQ, label-free quantitation. (**B**) Quantitative data were filtered using SignalP and literature searches to identify 67 of the total 191 proteins as secreted proteins. (**C**) Score plot of OPLS-DA showing the cluster separation between CTRL and LIRA-conditioned media samples. (**D**) Volcano plot of differentially expressed proteins for CTRL versus LIRA- conditioned media. Significantly ($P < 0.05$) and >2-fold differentially expressed proteins are displayed in green. Significantly differentially expressed proteins identified as secreted proteins are displayed in blue. $n = 3$ per group. False discovery rate < 0.05.

to latent structures discriminant analysis (OPLS-DA) displayed a clear cluster separation of conditioned media samples generated from saline-treated (CTRL) versus liraglutide-treated (LIRA) islets (Fig. 5C). Moreover, 13 proteins were found to be statistically ($P < 0.05$) and >2-fold differentially expressed between the CTRL- and LIRA-conditioned media samples (Fig. 5D).

To identify the protein factor mediating the increase in α cell PC1/3 expression in response to liraglutide, we prioritized proteins on the basis of the following criteria: (i) differential regulation in response to liraglutide treatment, (ii) classified as a factor secreted by β cells, and (iii) previously reported function in glucose homeostasis and GLP-1 biology. Only Ywhaz (hereafter: 14-3-3-zeta) matched all these criteria. 14-3-3-zeta was substantially decreased in conditioned media from liraglutide-treated islets (Fig. 5D), and a previous study found that whole-body KO of 14-3-3-zeta improves glucose regulation, which is ablated by administration of a GLP-1R antagonist (*35*). Therefore, we performed a series of studies to determine whether 14-3-3-zeta is involved in the effect of β cell GLP-1R signaling to activate α cell GLP-1 production.

To validate the proteomics findings and assess whether decreased secretion of 14-3-3-zeta in response to liraglutide was associated with a decrease in protein expression, we performed immunohistochemistry (IHC) on the isolated islets from β cell GLP-1R WT and KO mice studied as described above. Liraglutide treatment decreased 14-3-3-zeta area/islet compared to saline-treated mice in a β cell GLP-1R–dependent manner ($P < 0.01$; Fig. 6, A and B). These data, in combination with the untargeted proteomics data, suggest that liraglutide-induced β cell GLP-1R signaling decreases islet 14-3-3-zeta protein expression and secretion.

To assess the translational relevance of these findings, we performed targeted analysis of tryptic peptides of 14-3-3-zeta protein in conditioned media generated from nondiabetic human islets (fig. S4, A to C). Human islets were stimulated with 16.1 mM glucose + 100 nM liraglutide or saline for 15 min, and then conditioned media was collected, and targeted 14-3-3-zeta analysis of the digested samples was performed in duplicate. Liraglutide treatment resulted in a 25-fold decrease in 14-3-3-zeta abundance in the conditioned media from human islets, as compared to saline-treated controls (Fig. 6C). Similar results were obtained when this experiment was repeated in another human donor (fig. S4, D to F). IHC was then performed on human islets from three additional nondiabetic human donors (fig. S4G) that were treated with liraglutide (100 nM) or saline for 24 hours. Similar to the results in mouse islets, liraglutide treatment robustly decreased 14-3-3-zeta area/islet compared with saline-treated islets ($P < 0.01$; Fig. 6, D and E), demonstrating that the effect of liraglutide to decrease 14-3-3-zeta secretion and expression from mouse islets is translationally relevant in human islets.

To determine whether 14-3-3-zeta lowering contributes to the effect of β cell GLP-1R signaling to activate α cell GLP-1 expression, we applied pharmacologic addition and ablation of 14-3-3-zeta. Male and female WT mice were placed on HFD at 2 months of age for 12 to 19 weeks, after which, mice received saline or liraglutide treatment for 2 weeks and then were euthanized for islet isolation. Islets from liraglutide-treated mice were treated with media supplemented with liraglutide with and without recombinant 14-3-3-zeta. Comparatively, islets from saline-treated mice were incubated with and without the pan-14-3-3 inhibitor, R18 (*36*). Before experimentation in mouse islets, α TC1-6 cells were incubated in various

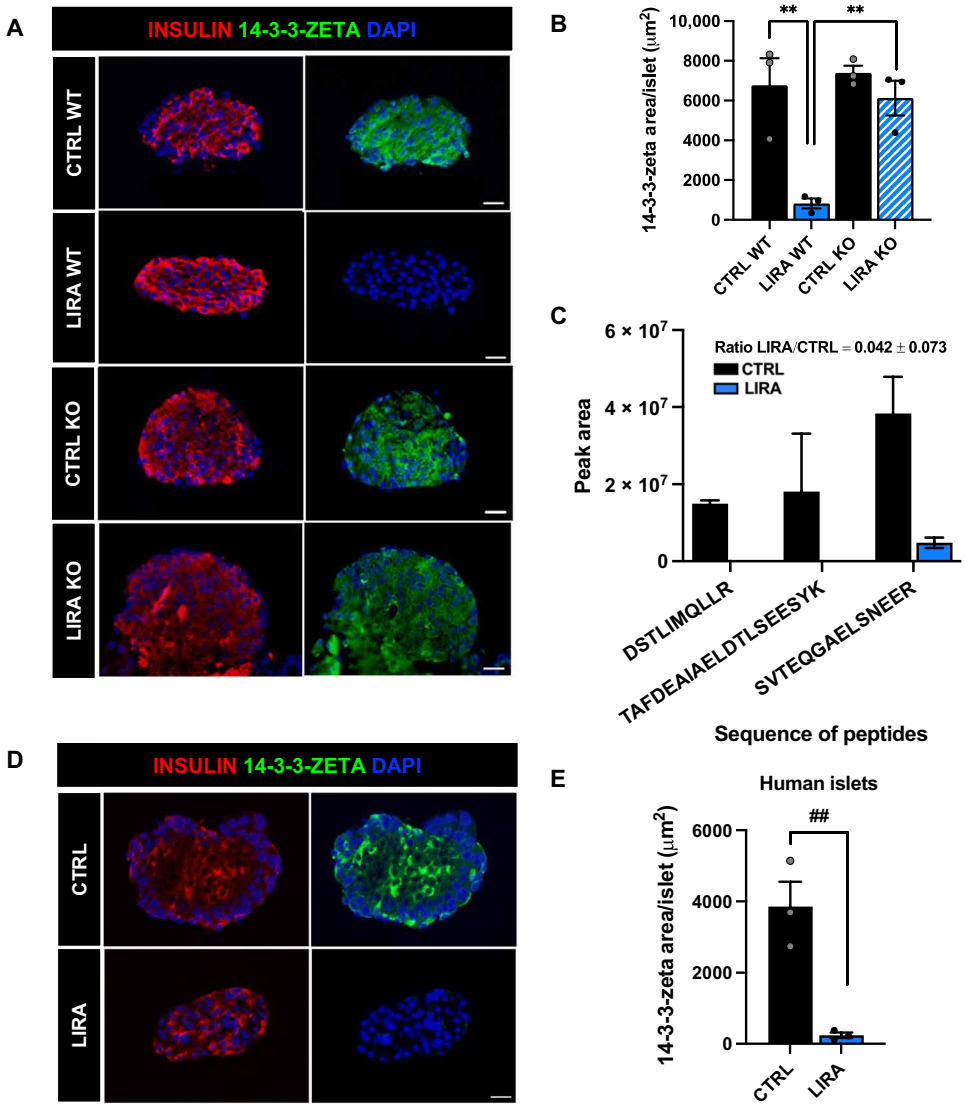

Fig. 6. Liraglutide decreases islet 14-3-3-zeta protein expression and secretion in mouse and human islets. (**A**) Representative images of mouse islets immunostained for insulin (red), 14-3-3-zeta (green), and DAPI (blue) in β cell GLP-1R WT and KO mice treated with saline (CTRL) or liraglutide (LIRA). (**B**) Average 14-3-3-zeta staining per islet in β cell GLP-1R WT and KO mice. (**C**) Abundance of four tryptic peptides of 14-3-3-zeta identified by targeted proteomics in conditioned media samples from human islets from a single human donor [human donor 1] treated with CTRL or LIRA, measured in duplicate. Ratio of abundance of the average of four tryptic peptides LIRA/CTRL is 0.042 ± 0.073. For the peptide TAFDEAIAELDTLSEESYK, both the 2+ and 3+ charge states (*z*) were quantified together. (**D**) Representative images of human islets treated with saline or liraglutide for 24 hours. Islets were immunostained for insulin (red), 14-3-3-zeta (green), and DAPI (blue). (**E**) Average 14-3-3-zeta staining per islet from human donors. Data are presented as means ± SEM. $n = 3$ donors/mice per group. $^{**}P < 0.01$ by two-factor ANOVA with Bonferroni's posttest; $^{\#\#}P < 0.01$ by Student's *t* test. Scale bar, 20 μm.

concentrations of recombinant 14-3-3-zeta and R18 for 24 hours. Recombinant 14-3-3-zeta and R18 did not affect α cell *Pcsk1* mRNA levels, demonstrating that these compounds on their own do not modulate α cell *Pcsk1* expression (fig. S5, A and B). In contrast, the addition of recombinant 14-3-3-zeta ablated the effect of conditioned media from liraglutide-treated islets to increase α cell *Pcsk1* mRNA expression ($P < 0.05$; Fig. 7A). Similarly, inhibition of 14-3-3 with R18 in saline-treated islets resulted in conditioned media that recapitulated the effect of conditioned media from liraglutide-treated islets to stimulate α cell *Pcsk1* expression ($P < 0.05$; Fig. 7A).

The same experimental paradigm was applied using the β TC clone-6 (β TC-6) β cell line to determine whether the impact of 14-3-3-zeta on α cell GLP-1 activation is β cell specific. β Cells were treated with liraglutide or saline for 14 days to mimic the effect of liraglutide dosing in vivo. β Cells were then stimulated with saline or liraglutide for 15 min, and conditioned media was placed on α cells. Similar to whole mouse islets, conditioned media from liraglutide-treated β cells increased α cell *Pcsk1* mRNA expression ($P < 0.05$; Fig. 7B), highlighting the β cell–specific nature of this effect. This effect was ablated by the addition of recombinant 14-3-3-zeta to liraglutide-treated β cells ($P < 0.05$; Fig. 7B). Furthermore, inhibition of 14-3-3 with R18 in saline-treated β cells resulted in conditioned media that mimicked the effect of conditioned media from liraglutide-treated β cells to increase α cell *Pcsk1* mRNA expression ($P < 0.05$;

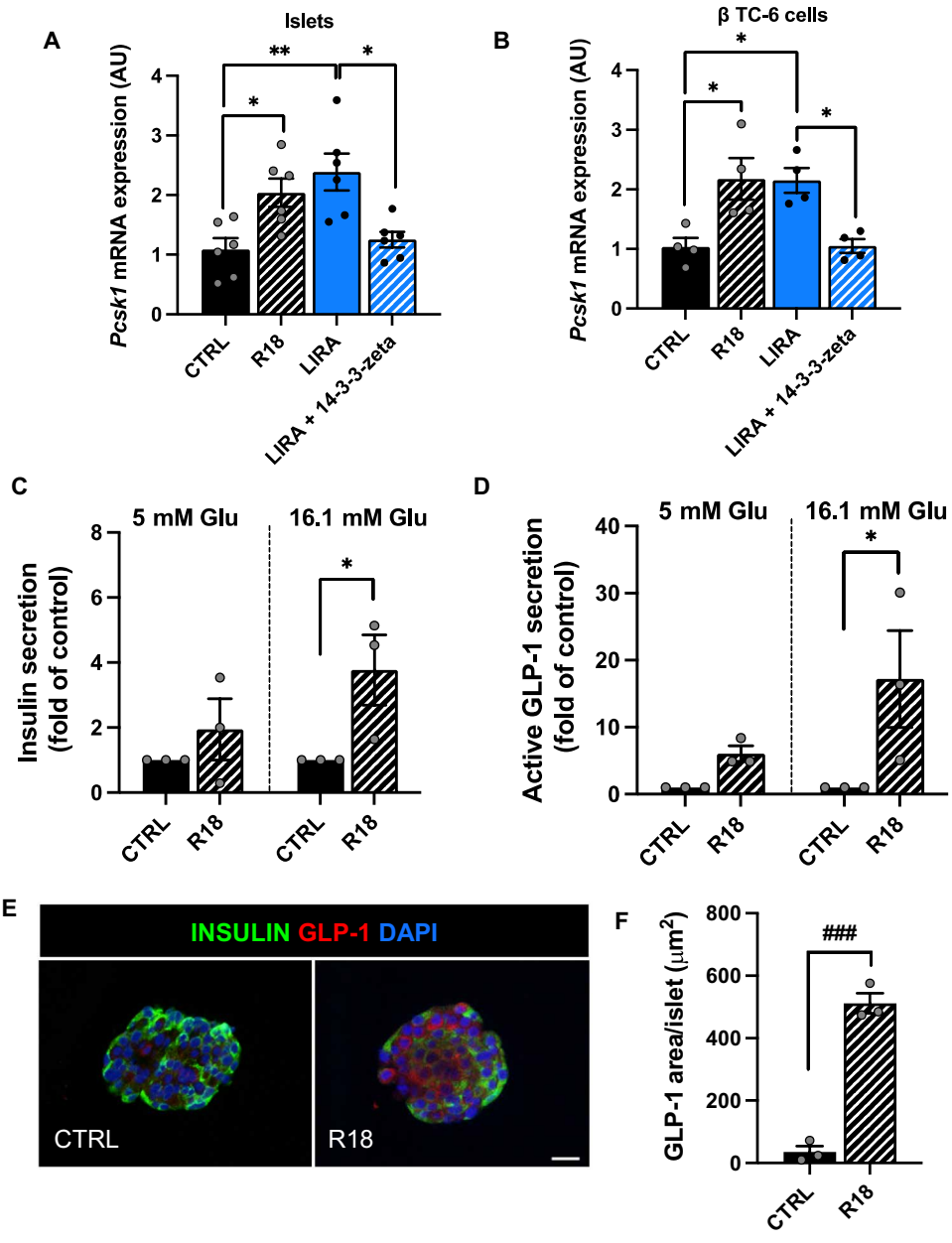

Fig. 7. Decreased 14-3-3-zeta mediates the effect of islet GLP-1R signaling to increase α cell PC1/3 expression and active GLP-1 secretion. (**A**) α Cell *Pcsk1* mRNA expression following treatment with conditioned media generated from islets of saline-treated WT mice following incubation with saline (CTRL) or R18, and liraglutide-treated WT mice following incubation with liraglutide (LIRA) or liraglutide + recombinant 14-3-3-zeta. (**B**) α Cell *Pcsk1* mRNA expression following 24-hour treatment with conditioned media generated from β cells treated with saline, R18, liraglutide, or liraglutide +14-3-3-zeta. (**C**) Insulin and (**D**) active GLP-1 secretion from human islets incubated with R18 or saline under low-glucose (5 mM) and high-glucose (16.1 mM) conditions. (**E**) Representative images of human islets treated with saline or R18 for 24 hours. Islets were immunostained for insulin (green), GLP-1 (red), and DAPI (blue). (**F**) Average GLP-1 staining per islet from human donors. Data are presented as means ± SEM. $n = 3$ to 6 per group. *$P \leq 0.05$, **$P < 0.01$ by one-factor or two-factor ANOVA with Bonferroni's posttest. ###$P < 0.001$ by Student's t test. Scale bar, 20 μm. AU, arbitrary units.

Fig. 7B). These data suggest that 14-3-3-zeta inhibits a protein secreted in response to β cell GLP-1R signaling that can activate α cell GLP-1 expression.

To assess the translational relevance of these findings, human islets from nondiabetic donors (fig. S4G) were incubated in 16.1 mM glucose supplemented with R18 (2 μM) or saline for 24 hours. Following this 24-hour incubation, islets were serum- and low glucose (5 mM)–starved for 1 hour and then incubated in high glucose (16.1 mM) or low glucose (5 mM) media supplemented with and without R18 for 15 min followed by conditioned media collection. Consistent with a relationship to the incretin effect, R18 increased insulin secretion under high-glucose but not low-glucose conditions ($P \leq 0.05$; Fig. 7C). These findings are consistent with results from a recent study (*37*). Moreover, R18 treatment resulted in a glucose-dependent increase in islet-active GLP-1 secretion, as compared to saline-treated controls ($P < 0.01$; Fig. 7D). In parallel, a separate set of islets from

the same donors were treated with R18 (2 μM) or saline for 24 hours, after which, islets were fixed and sectioned for IHC and costained for insulin and GLP-1. Similar to our previous findings regarding the effect of liraglutide treatment on human islets (*21*), R18 treatment increased islet GLP-1 expression, as compared to saline-treated controls ($P < 0.001$; Fig. 7, E and F). Together, these findings demonstrate that 14-3-3 inhibition increases GSIS and active GLP-1 secretion from human islets.

DISCUSSION

Here, we define the bidirectional paracrine cross-talk between α and β cells that contribute to the glucoregulatory effect of a GLP-1R agonist. First, we find that the effect of liraglutide to increase islet GLP-1 expression, improve glucose tolerance, and increase insulin secretion is dependent on the β cell GLP-1R. Furthermore, we find that the effect of liraglutide to induce islet GLP-1 expression is dependent on α cells and that α cells contribute to the effect of liraglutide to improve glucose tolerance and GSIS in response to intraperitoneal glucose in male mice. In parallel, we find that the effect of enhanced β cell GLP-1R signaling to activate α cell GLP-1 production is mediated by a secreted protein factor. Our data show that activation of β cell GLP-1R signaling by a GLP-1R agonist reduces expression and secretion of 14–3-3-zeta. This decrease in 14-3-3-zeta is necessary for subsequent activation of α cell GLP-1 production. Together, our results refine our understanding of β cell GLP-1R function and identify 14-3-3-zeta as a potential target with which to enhance α cell GLP-1 production.

The present findings build upon recent studies that have documented the importance of α cell paracrine signaling for healthy insulin secretory dynamics and normal islet function (*16*, *18*–*20*, *38*). This work builds upon these previous studies by manipulating both the β cell GLP-1R and the α cell in vivo and is the first to assess the role of the α cell in the metabolic effects of a GLP-1R agonist. Previous studies have shown that mice with α cell ablation exhibit no impairment of the counterregulatory response to prolonged starvation and insulin-induced hypoglycemia (*25*); however, it is possible that α cell ablation results in compensatory increases in other glucose-mobilizing and glucose-disposing pathways enabling normal glycemic control. In addition, previous studies have documented hyperaminoacidemia and impaired amino acid metabolism in animal models with glucagon deficiency (*39*–*41*). Hence, it is possible that altered amino acid metabolism contributes to the metabolic phenotype of mice with α cell ablation in the present studies. Despite these limitations, the data generated from this approach demonstrate that the effect of a GLP-1R agonist to enhance α cell GLP-1 expression is blunted by β cell GLP-1R KO and α cell ablation in mice. Furthermore, the effect of a GLP-1R agonist to augment GSIS is blunted by α cell ablation in male mice. Previous studies have documented sex-related differences in the glycemic response to liraglutide in humans, in which females exhibited a greater reduction in HbA1c levels as compared to males (*42*). Moreover, progesterone and estrogen have been shown to enhance GLP-1 secretion from mouse (*43*, *44*) and human (*44*) α cells and L cells in vitro, highlighting the potential for sex-dependent differences in the regulation of GLP-1 secretion. Nevertheless, considering that liraglutide increases α cell GLP-1 secretion and decreases glucagon secretion (*45*), and that GLP-1 is 300-fold more potent at stimulating β cell GLP-1R–induced GSIS than glucagon (*18*, *46*), these findings may reflect the loss of paracrine signaling by α cell–derived GLP-1. However, the use of α cell ablation does not specifically modulate GLP-1, and further studies are needed to evaluate the role of α cell GLP-1 in the metabolic effects of GLP-1R agonist treatment.

The present findings underscore the glucoregulatory importance of β cell GLP-1R signaling under HFD-fed conditions, in that glucose tolerance is impaired in saline-treated β cell GLP-1R KO mice compared with WT mice during the OGTT. This is in contrast to a previous study that reported that β cell GLP-1R KO does not affect oral glucose tolerance compared to WT controls when mice are maintained on a low-fat diet (*29*). Metabolic stress has been reported to decrease L cell–derived GLP-1 and increase α cell–derived GLP-1 in rodents and humans (*8*, *10*–*12*, *47*–*51*), suggesting that there may be an increased reliance on α cell GLP-1 under metabolic stress. For example, work in an α cell–specific PC1/3 KO mouse model demonstrates that the loss of α cell GLP-1 production impairs glucose homeostasis and GSIS in metabolically stressed mice but not in chow-fed mice (*20*). Furthermore, islets from type 2 diabetic human donors display an increased subpopulation of GLP-1$^+$ α cells and a greater dependency on GLP-1R signaling for insulin secretion, as compared to islets from healthy donors (*5*). Further work is needed to define the relative contributions of the α and L cells to β cell GLP-1R function in health and metabolic disease.

In parallel, we sought to elucidate the β-to-α cell paracrine signaling mechanisms regulating α cell GLP-1 production. The present findings indicate that the effect of β cell GLP-1R signaling to increase α cell PC1/3 expression is mediated by secreted protein factors that act in a paracrine fashion. Subsequent characterization and identification of the proteome secreted by islets in response to liraglutide and saline revealed 14-3-3-zeta as a lead candidate in the regulation of α cell GLP-1 production. These studies suggest that enhanced β cell GLP-1R signaling decreases the production and secretion of 14-3-3-zeta, which then enables activation of α cell–active GLP-1 production and secretion.

14-3-3-zeta is an isoform of the 14-3-3 protein family. The 14-3-3 proteins serve as molecular adaptors that bind to phosphorylated proteins with phosphoserine and phosphothreonine motifs (*36*, *52*). The 14-3-3 proteins bind to various target proteins and function as allosteric modulators by inducing conformational changes in target proteins, modulating target protein activity and stability, bridging protein complex formation, or by altering protein subcellular localization (*53*–*57*). Through these functions, 14-3-3 proteins have been implicated as key regulators in glucose metabolism (*58*–*60*).

One of the mechanisms by which 14-3-3-zeta is thought to influence glucose regulation is through modulation of pancreatic islet function; however, the pathways mediating the effects of 14-3-3-zeta on islet function have been unclear. A previous study found that whole-body ablation of 14-3-3-zeta improves glucose regulation in mice and that treatment of 14-3-3-zeta KO mice with the GLP-1R antagonist exendin 9-39 attenuated the glucoregulatory improvements associated with whole-body 14-3-3-zeta ablation (*35*). Furthermore, a recent study found that β cell–specific 14-3-3-zeta ablation enhances GSIS in mice (*37*). Similarly, treatment of human islets with pan-14-3-3 inhibitors increases GSIS (*37*). These data suggest that 14-3-3-zeta serves as a negative regulator of insulin secretion in human and mouse islets. Consistent with this notion, previous work has shown that 14-3-3-zeta expression increases in models of overt diabetes in mice, and this is associated with a decreased expression of *Ins1* and *Ins2*, as well as β cell maturity markers, *MafA* and *Pdx*-1

(*37*, *61*). However, prolonged treatment with 14-3-3 inhibitors can increase expression of these genes to nondiabetic levels (*37*). The effects of GLP-1R agonist treatment parallel these effects of 14-3-3-zeta ablation. GLP-1R agonist treatment enhances GSIS and increases expression of markers of β cell maturity (*62*–*64*). Our results suggest that the effect of 14-3-3-zeta inhibition to improve GSIS is mediated by an increase in α cell GLP-1 production and secretion.

Our results demonstrate that 14-3-3-zeta inhibition can alter α cell proglucagon processing, which is similar to previous studies that have identified a role for 14-3-3-zeta in the regulation of gut-derived GLP-1 production. KO of 14-3-3-zeta in the GLUTag L cell line has been shown to increase GLP-1 content (*35*). Here, we demonstrate that β cell GLP-1R signaling activates α cell GLP-1 expression by decreasing β cell 14-3-3-zeta production and secretion. We hypothesize that under unstimulated conditions, 14-3-3-zeta binds to and inactivates a protein that can stimulate α cell GLP-1 production. 14-3-3-zeta is found in β cell secretory granules (*59*), suggesting that under unstimulated conditions, 14-3-3-zeta exerts its inhibitory function within a secretory granule; however, further work is needed to define the dynamics and cellular location of this interaction. Upon pharmacologic β cell GLP-1R stimulation, β cell 14-3-3-zeta expression is down-regulated, which likely releases this protein from inhibition such that it can act in a paracrine manner to activate α cell GLP-1 production. Further studies investigating the proteins that interact with 14-3-3-zeta in the β cell are needed. Moreover, while our results suggest that liraglutide suppresses 14-3-3-zeta protein expression within the islet in a β cell GLP-1R–dependent manner, future work is needed to define the β cell GLP-1R signaling cascade that directly mediates 14-3-3-zeta secretion. Furthermore, because 14-3-3-zeta is found in GLP-1R–expressing cell types other than β cells, it will be of interest to determine the role of 14-3-3-zeta in GLP-1R signaling in other cell types. Nevertheless, the present findings are the first to demonstrate that 14-3-3-zeta production and secretion are regulated by β cell GLP-1R signaling, that 14-3-3-zeta is a downstream regulatory of GLP-1R function, and that 14-3-3-zeta regulates α cell proglucagon processing.

In conclusion, these data reveal a role for the α cell in the glucoregulatory effects of a GLP-1R agonist and a previously unknown role for β cell GLP-1R signaling in decreasing 14-3-3-zeta expression to activate α cell GLP-1 production. These studies deepen our understanding of the regulation of α cell GLP-1 production and GLP-1R agonist function, which may facilitate development of improved therapies for diabetes treatment.

MATERIALS AND METHODS

Animals, diet, and islets

In vivo assessment of glucose tolerance

For all studies, mice were individually housed and maintained in a temperature- and humidity-controlled room, with a 14-/10-hour light-dark cycle. Body weights were matched between groups at the start of liraglutide and saline treatment for all studies. The experimental protocols were approved by the Cornell University Institutional Animal Care and Use Committee.

To assess the role of the β cell GLP-1R on islet GLP-1 expression and oral glucose tolerance, we studied tamoxifen-inducible β cell–specific GLP-1R WT and KO mice (*21*). To assess whether the glucoregulatory benefits of liraglutide are dependent, at least in part, on α cells, we used tamoxifen-inducible β cell–specific GLP-1R WT mice (*21*) crossed to a DT-inducible mouse model of α cell ablation (*GcgDTR*), provided by M. Donath (*25*). For these studies, at 7 to 9 weeks of age, male and female *GcgDTR*$^{-}$*-Glp-1r*$^{\beta\,cell+/+}$ [*MIPCreERT*$^{-}$*-hGlp-1r*] and *GcgDTR*$^{-}$*-Glp-1r*$^{\beta\,cell-/-}$ [*MIPCreERT*$^{+}$*-hGlp-1r*] littermates and male and female *GcgDTR*$^{+}$*-Glp-1r*$^{\beta\,cell+/+}$ [*MIPCreERT*$^{-}$*-hGlp-1r* with *GcgDTR*$^{+}$] littermates were placed on HFD consisting of ground chow (Teklad 2018, Envigo; Madison, WI) supplemented with 3.4% butter fat, 8.5% tallow, 13.1% soybean oil, 3.5% mineral mix, and 1% vitamin mix (Dyets, Bethlehem, PA) for 8 to 10 weeks. Mice were switched to an HFD with diet tamoxifen citrate (TD.710935, 400 mg tamoxifen citrate/kg of diet; Envigo, Madison, WI) for the duration of the study to induce and maintain GLP-1R KO. DT injections were administered (504 ng; intraperitoneal) (D0564, Sigma-Aldrich; St. Louis, MO) to all mice on days 1, 3, and 5 of the start of HFD with tamoxifen, as previously validated (*20*). Two weeks after the start of HFD with tamoxifen, mice were given twice daily (08:00 and 16:00) subcutaneous injections of either saline or liraglutide (200 μg/kg of body weight, subcutaneous) (HY-P0014, MedChemExpress, Monmouth Junction, NJ) for 3 weeks. Following 2 weeks of liraglutide/saline treatment, mice were fasted overnight (12 hours), and an OGTT (2 g/kg body weight oral gavage with dextrose) was performed, as previously described (*32*). One week later (3 weeks after the start of liraglutide/saline treatment), mice were fasted overnight (12 hours), and an IPGTT (2 g/kg body weight intraperitoneal injection with dextrose) was performed, as previously described (*30*). For both the OGTT and IPGTT, liraglutide or saline was administered 15 min before the glucose bolus, as previously described (*29*, *30*). Glucose measurements were made using a glucometer (One-Touch Ultra, Lifescan, Malvern, PA). Immediately following the IPGTT, mice were euthanized by an overdose of pentobarbital (200 mg/kg of body weight, intraperitoneal), and tissues were weighed and collected. Serum glucagon and insulin were measured by enzyme-linked immunosorbent assay (ELISA) (glucagon: Mercodia, Winston Salem, NC; insulin: Millipore, Billerica, MA). Area under the curve (AUC) for blood glucose and serum insulin concentrations were calculated using the trapezoidal method. Insulin secretion index was calculated as $\mathrm{InsulinAUC}_{(0-30)}/\mathrm{GlucoseAUC}_{(0-30)}$ during the OGTT and IPGTT, as previously described (*65*–*69*).

For assessment of the effect of MIP-CreERT in our model (fig. S3), male and female *Cre*$^{-}$ (*MIPCreERT*$^{-}$*-hGlp-1r*) and *Cre*$^{+}$ (*MIPCreERT*$^{+}$*-hGlp-1r*) littermates were given ad libitum access to HFD consisting of ground chow supplemented with 3.4% butter fat, 8.5% tallow, 13.1% soybean oil, 3.5% mineral mix, and 1% vitamin mix for 8 weeks. After 8 weeks, mice were switched to a synthetic HFD (TD.08840, Envigo, Madison, WI) and pair-fed to match the food intake of the *Glp-1r*$^{\beta\,cell+/+}$ mice on the tamoxifen-HFD to control for the effect of tamoxifen to reduce food intake. Two weeks after the start of pair feeding, mice were treated with saline or liraglutide for 2 weeks, and an OGTT was performed, as described above. One week later (3 weeks after the start of liraglutide/saline treatment), an IPGTT was performed, as described above.

In vitro assessment of β cell GLP-1R signaling on α cell PC1/3 expression

To assess whether β cell GLP-1R signaling causes secretion of a factor that acts in a paracrine manner to increase α cell PC1/3 expression (Fig. 4, C to E, and H and I), at 8 to 11 weeks of age, male and female *Glp-1r*$^{\beta\,cell+/+}$ and *Glp-1r*$^{\beta\,cell-/-}$ littermates were placed on HFD for 8 to 10 weeks. All mice received subcutaneous injections of tamoxifen (200 mg/kg body weight; T5648, Sigma-Aldrich, St. Louis, MO)

starting after 8 to 10 weeks of HFD feeding (three doses over 5 days). Following the final tamoxifen injection, mice received injections of either saline or liraglutide for 2 weeks, as described above. Following 2 weeks of liraglutide or saline treatment, mice were fasted overnight (12 hours) and given their last dose of liraglutide or saline at 08:00. Two hours after the final dose of liraglutide or saline, mice were euthanized by an overdose of pentobarbital (200 mg/kg body weight, intraperitoneal), and pancreatic islets were isolated. Mouse islets were isolated after collagenase digestion, filtration, Histopaque gradient, and handpicking, as previously described (*23*). Islets were cultured overnight (37°C, 5% CO_2) in RPMI 1640 media with 11.1 mM glucose, 1% antibiotic-antimycotic, and 10% (v/v) fetal bovine serum (FBS) to allow islets to rest before experimentation.

Following the overnight rest, islets were serum-starved in RPMI 1640 with 2.8 mM glucose for 2 hours. Islets were handpicked into six-well culture plates (10 islets per well) and incubated in RPMI 1640 with 11.1 mM glucose supplemented with 100 nM liraglutide (S8256, Selleckchem; Radnor, PA) or saline for 15 min or 2 hours. At each of these time points, conditioned media was collected and applied to α TC1-6 cells at a dilution of 1:2.7. In addition, to assess α cell–active GLP-1 secretion in response to treatment with islet-conditioned media, the conditioned media from islets from a subset of these mice was passed through Amicon ultracentrifugal filters (Millipore, Billerica, MA) with a molecular weight cutoff of 50 kDa to remove liraglutide, proglucagon-derived products, and insulin from the conditioned media (Fig. 4, H and I). Following this filtration, the conditioned media were diluted in RPMI 1640 with 11.1 mM glucose to return to the starting glucose concentration and were then applied to α TC1-6 cells at a dilution of 1:2.7. Insulin secretion in response to culture in 100 nM liraglutide or saline was measured in islet-conditioned media from the 15-min time point using an insulin ELISA (ALPCO, Salem, NH).

In vitro characterization of β cell paracrine signaling factors

To define key characteristics of the paracrine factor that signals to α cells to increase PC1/3 expression and GLP-1 production (Fig. 4, F and G), at 7 to 8 weeks of age, male and female WT mice were placed on HFD for 8 weeks. Following 8 weeks of HFD feeding, mice received injections of either saline or liraglutide for 2 weeks, as described above. Following 2 weeks of liraglutide or saline treatment, mice were euthanized, and islets were isolated as described above.

Following the overnight rest, islets were serum-starved in RPMI 1640 with 2.8 mM glucose for 2 hours. Islets were handpicked into six-well culture plates (10 islets per well) and incubated in RPMI 1640 with 11.1 mM glucose supplemented with 100 nM liraglutide or saline for 15 min or 2 hours. At each of these time points, conditioned media was collected and applied to α TC1-6 cells at a dilution of 1:2.7.

In addition, subaliquots of conditioned media from the 15-min time points were subjected to PK (Qiagen, Germantown, MD) treatment, a freeze-thaw cycle, or fractionation based on molecular weight before addition to α TC1-6 cells at a 1:2.7 dilution. For the PK treatment, conditioned media was treated with PK (100 μg/ml) and incubated at 56°C for 30 min. PK activity was inactivated by incubation of samples at 95°C for 10 min, followed by cooling to 37°C. For the freeze-thaw treatment, conditioned media was frozen at −80°C for at least 24 hours, defrosted, and warmed to 37°C. For the molecular weight fractionations, conditioned media was fractionated through Amicon ultracentrifugal filters (Millipore, Billerica, MA) with a molecular weight cutoff of 50 kDa. The resulting concentrate, containing the fraction greater than 50 kDa, and the filtrate, containing the fraction less than 50 kDa, were diluted in RPMI 1640 with 11.1 mM glucose to return to the starting concentration and were then applied to α TC1-6 cells at a dilution of 1:2.7.

Proteomics analysis of islet-conditioned media

To define the paracrine protein factor(s) responsible for the effect of β cell GLP-1R signaling to increase α cell GLP-1 production, islet-conditioned media was generated for proteomics analysis. Mice were studied as described above, except mice were on HFD for 9 to 10 weeks before saline or liraglutide treatment. Following 2 weeks of liraglutide or saline treatment, mice were euthanized, and islets were isolated as described above.

Following the overnight rest, islets were serum-starved in RPMI 1640 with 2.8 mM glucose for 2 hours. Islets were then handpicked into 12-well culture plates (125 islets per well) and incubated in RPMI 1640 with 11.1 mM glucose supplemented with 100 nM liraglutide or saline for 15 min. Conditioned media was treated with 1x Halt Protease Inhibitor Cocktail (Thermo Fisher Scientific, Waltham, MA) and fractionated using Amicon ultracentrifugal filters with a molecular weight cutoff of 50 kDa. The greater than 50-kDa fraction was submitted for analysis.

In vitro functional validation of 14-3-3-zeta in mice

To determine whether 14-3-3-zeta contributes to the effect of β cell GLP-1R signaling to activate α cell GLP-1 expression, 8-week-old male and female WT mice were placed on HFD for 12 to 19 weeks, after which, mice received injections of either saline or liraglutide for 2 weeks. Following 2 weeks of liraglutide or saline treatment, mice were euthanized, and islets were isolated as described above.

Islets were handpicked into six-well culture plates (10 islets per well) and allowed to rest overnight. During the overnight rest, a subset of islets from saline-treated mice were treated with 2 μM R18 (Tocris, Minneapolis, MN) for 24 hours. Following this treatment and the overnight rest, all islets were serum-starved in RPMI 1640 with 2.8 mM glucose for 2 hours. Islets from liraglutide-treated mice were incubated in RPMI 1640 with 11.1 mM glucose supplemented with 100 nM liraglutide with or without 10 nM of recombinant mouse 14-3-3-zeta (ab268301, Abcam, Cambridge, MA) for 15 min before the collection of conditioned media. In addition, islets from saline-treated mice were treated with RPMI 1640 with 11.1 mM glucose supplemented with saline for 15 min before the collection of conditioned media. R18-treated islets from saline-treated mice were then incubated in RPMI 1640 with 11.1 mM glucose supplemented with 2 μM R18 for 15 min before the collection of conditioned media. For each of these conditions, conditioned media was collected and applied to α TC1-6 cells at a dilution of 1:2.7.

To control for the effect of 14-3-3-zeta and R18 on α cell *Pcsk1* expression, a dose response was performed in α TC1-6 cells in which 1, 10, and 100 nM recombinant mouse 14-3-3-zeta and 0.02, 0.2, and 2 μM R18 were added to α TC1-6 cells in the absence of islet-conditioned media and incubated for 24 hours. Concentrations of R18 and 14-3-3-zeta were selected on the basis of previous in vitro assays (*70*, *71*) and the reported dissociation constant of R18 at 80 nM (*72*).

α Cell culture

α TC1-6 [American Type Culture Collection (ATCC) CRL-2934] cells were purchased from ATCC (Manassas, VA). α TC1-6 cells were

cultured in Dulbecco's modified Eagle's media (DMEM) supplemented with 10% (v/v) heat-inactivated FBS, 1% antibiotic-antimycotic, 15 mM Hepes, 6 mM L-glutamine, 0.1 mM nonessential amino acids, 0.02% bovine serum albumin (BSA), sodium bicarbonate (1.5 g/liter), and 11.1 mM glucose at 37°C and 5% CO_2. α TC1-6 cells at 10 to 20 passages were used in all experiments described below. Cells were seeded at 395,000 cells/cm^2. Before treatment with conditioned media generated from islets, α TC1-6 cells were serum-starved in DMEM supplemented with 15 mM Hepes, 6 mM L-glutamine, 0.1 mM nonessential amino acids, sodium bicarbonate (1.5 g/liter), and 11.1 mM glucose (referred to as serum-free α cell media) for 2 hours. For all conditioned media studies described above, islet-conditioned media was applied to α TC1-6 cells at a ratio of 1 (islet-conditioned media): 2.7 (serum-free α cell media), and α TC1-6 cells were incubated in the islet-conditioned media for 24 hours.

For all experiments, following 24 hours of incubation in islet-conditioned media, media from α TC1-6 cells was collected and treated with 125 μM dipeptidyl peptidase IV (DPP-IV) inhibitor (Millipore, Billerica, MA) and aprotinin (500K IU/ml; Sigma-Aldrich, St. Louis, MO), and then, cells were washed with phosphate-buffered saline (PBS), and total RNA (*73*) or protein was isolated. RNA was converted into complementary DNA (cDNA) with the iScript cDNA Synthesis Kit (Bio-Rad, Hercules, CA). Gene expression was assessed by quantitative polymerase chain reaction using SYBR Green detection, and threshold values were normalized to the expression of β-actin. Primer sequences were as follows: β-actin 5′-3′ CAACGAGCGGTTCCGAT, 3′-5′ GCCACAGGATTCCATACCCA; *Pcsk1* 5′-3′ CTCTGGTGGATTTGGCTGAT, 3′-5′ GGGCTCTAGGCTCAAAGTTATT. Proteins from α TC1-6 cells were extracted using radioimmunoprecipitation assay buffer [10 mM tris-HCl (pH 7.4), 150 mM NaCl, 0.1% SDS, 1% Triton X-100, 1% sodium deoxycholate, 5 mM EDTA, 1 mM NaF, 1 mM sodium orthovanadate, protease inhibitors, and 125 μM DPP-IV inhibitor] and quantified with the bicinchoninic acid protein assay kit (Pierce, Thermo Fisher Scientific, Waltham, MA). Active GLP-1 content in protein lysates from α TC1-6 cells and active GLP-1 secretion in conditioned media from α TC1-6 cells treated with greater than 50-kDa islet-conditioned media fractions were measured by sandwich electrochemiluminescence immunoassay (Meso Scale Discovery, Kenilworth, NJ). Active GLP-1 protein concentrations were normalized to the total protein content in cell lysates.

β Cell culture

β TC-6 (ATCC CRL-11506) cells were purchased from ATCC. In the β cell experiments, α cells were cultured as described above. β TC-6 cells were cultured in DMEM with 5.5 mM glucose and 15% (v/v) heat-inactivated FBS and 1% antibiotic-antimycotic at 37°C and 5% CO_2. β TC-6 cells were studied between passages 4 and 6. Before conditioned media studies, β TC-6 cells were treated with PBS or liraglutide (100 nM) for 2 weeks. To generate β TC-6 cell–conditioned media, cells were seeded at 395,000 cells/cm^2. A subset of PBS-treated β TC-6 cells were treated with 2 μM R18 for 24 hours. β TC-6 cells were serum-starved in DMEM supplemented with 5.5 mM glucose for 2 hours. Following serum starvation, β TC-6 cells previously treated with PBS were incubated in DMEM supplemented with 11.1 mM glucose for 15 min, and β TC-6 cells treated with R18 were incubated in DMEM supplemented with 11.1 mM glucose with 2 μM R18 for 15 min. β TC-6 cells previously treated with liraglutide were incubated in DMEM supplemented with 11.1 mM glucose and 100 nM liraglutide with and without 10 nM of mouse recombinant 14-3-3-zeta for 15 min. Following these 15-min incubations, conditioned media was collected and applied to α TC1-6 cells at a dilution of 1:2.7.

IHC and image analysis

Pancreas sections from mice studied as described above were further analyzed by IHC, as previously described (*21*, *22*, *32*). β Cell GLP-1R WT islets used for the generation of conditioned media analyzed by proteomics, β cell GLP-1R KO islets from conditioned media studies, and human islets from three separate donors treated as described below were washed, fixed, collected in HistoGel (Epredia, Kalamazoo, MI), and paraffin-embedded, as previously described (*21*). For both mouse and human islets, as well as mouse pancreas sections, after embedding in paraffin, 5 μM sections were cut for IHC. Samples were deparaffinized in xylene and rehydrated in serial ethanol dilutions. Antigen retrieval was performed for 20 min in boiling tris-EDTA (pH 9). Blocking was performed with 5% BSA. Mouse and human islet sections were immunostained for insulin using a monoclonal anti-mouse antibody (1:200; SC-377071, Santa Cruz Biotechnology, Dallas, TX) and for 14-3-3-zeta using a monoclonal anti-rabbit antibody (1:50; CS-7413, Cell Signaling Technology, Danvers, MA). Separate human islet sections were immunostained for GLP-1 using a monoclonal anti-mouse antibody (1:100; ab26278, Abcam, Cambridge, MA) and for insulin using a polyclonal anti-rabbit antibody (1:200; SC-9168, Santa Cruz Biotechnology). Mouse pancreas sections were immunostained for GLP-1 (same as above) and for glucagon using a polyclonal anti-rabbit antibody (SC-7779R; Santa Cruz Biotechnology; 1:200). Detection of primary antibodies was performed with Alexa Fluor 488 anti-rabbit (A11034) and Alexa Fluor 633 anti-mouse (A21052) secondary antibodies (1:200; Invitrogen, Foster City, CA). Nuclei were detected with 4′,6′-diamidino-2-phenylindole [Invitrogen (P36962)].

Mouse pancreas image quantification and analysis were performed on all islets in a single longitudinal cross section of the pancreas, as previously described (*21*) (1 cross section per mouse; 22 islets per mouse on average for GLP-1 and 10 islets per mouse for glucagon). Mouse and human islet image quantification and analysis were performed on 5 μM slices of individual islets sectioned through the center of the islet (eight islet sections per mouse on average, six islet sections per human on average). Islet imaging and quantification were performed in a blinded fashion. Islets were manually traced and quantified using ImageJ software. Islets were imaged using a Nikon Eclipse E400 fluorescent microscope with Olympus DP73 color camera.

Human islet–conditioned media and processing

Nondiabetic human islets were obtained from the Integrated Islet Distribution Program. Human donor information is listed in fig. S4. Upon arrival, islets were cultured for approximately 36 hours (37°C, 5% CO_2) in RPMI 1640 with 16.1 mM glucose, 1% antibiotic-antimycotic, and 10% (v/v) FBS. For the generation of conditioned media used for targeted proteomics analyses, after approximately 36 hours, islets were handpicked into serum-free media (RPMI 1640 with 16.1 mM glucose) for 2 hours. After 2 hours, islets were handpicked into six-well plates (500 islets per well) and incubated in RPMI 1640 with 16.1 mM glucose supplemented with 100 nM liraglutide or saline for 15 min. Conditioned media from the islets was collected after 15 min and treated with 1x Halt Protease Inhibitor Cocktail (Thermo Fisher Scientific, San Jose, CA) and concentrated

at 14,000*g* using Amicon ultracentrifugal filters (Millipore, Billerica, MA) with a molecular weight cutoff of 3 kDa.

For the human islets used for IHC, islets were cultured and serum-starved as described above. Following 2-hour serum-starving, islets were handpicked into 48-well plates (63 islets per well) and incubated in RPMI 1640 with 16.1 mM glucose supplemented with 100 nM liraglutide, or 2 μM R18, or saline for 24 hours. After the 24-hour incubation, islets were washed, fixed, collected in HistoGel, and paraffin-embedded, as previously described (*21*).

To determine the translational relevance of the effect of 14-3-3-zeta inhibition to increase α cell PC1/3 expression, islets from the same human donors used for IHC were cultured as described above. Following 36 hours of culture, islets were handpicked into 48-well plates (63 islets per well) and incubated in RPMI 1640 with 16.1 mM glucose, 1% antibiotic-antimycotic, and 10% (v/v) FBS and supplemented with either 2 μM R18 or saline for 24 hours. After the 24-hour incubation, islets were serum- and low-glucose– (RPMI 1640 with 5 mM glucose) starved for 1 hour, after which, islets were incubated in either high-glucose (RPMI 1640 with 16.1 mM glucose) or low-glucose (RPMI 1640 with 5 mM glucose) media supplemented with 2 μM R18 or saline for 15 min. Conditioned media from the islets was collected after 15 min and treated with 1x Halt Protease Inhibitor Cocktail, as well as 125 μM DPP-IV inhibitor and aprotinin (500K IU/ml). Insulin and active GLP-1 content in protein lysates and secretion in conditioned media were measured by ELISA for insulin (ALPCO, Salem, NH) and by a sandwich electrochemiluminescence immunoassay for active GLP-1 (Meso Scale Discovery, Kenilworth, NJ). Insulin and active GLP-1 secretion were normalized to the total insulin and total active GLP-1 cell content (protein content in cell lysates plus conditioned media), respectively, and expressed as a fold of control (*74*).

Proteomics

Protein concentration was determined by SDS–polyacrylamide gel electrophoresis with a known concentration of *Escherichia coli* proteins as a standard. In-solution digestion of 5 μg of protein was performed on S-Trap micro spin column (ProtiFi, Huntington, NY, USA) following an S-Trap protocol, as described previously (*75*, *76*). The tryptic digests were reconstituted for nano liquid chromatography (LC)–electrospray ionization tandem mass spectrometry (MS/MS) analysis, as previously described (*75*). As an internal standard, enolase (yeast) tryptic digests were added to each sample in the final concentration of 2.5 fmol/μl. The analysis was carried out using an Orbitrap Fusion Tribrid (Thermo Fisher Scientific, San Jose, CA) mass spectrometer equipped with a nanospray Flex Ion Source and coupled with a Dionex UltiMate 3000 RSLCnano system (Thermo Fisher Scientific, Sunnyvale, CA) using parameters as previously outlined (*75*, *77*). The peptide samples (20 μl) were injected onto a PepMap C-18 RP nano trapping column and eluted in a 120-min gradient, as previously described (*75*). All data were acquired under Xcalibur 4.4 operation software (Thermo Fisher Scientific).

For the untargeted proteomics of mouse conditioned media samples, the data-dependent acquisition (DDA) raw files for collision-induced dissociation MS/MS were subjected to database searches using Proteome Discoverer (PD) 2.4 software (Thermo Fisher Scientific, Bremen, Germany) with the Sequest HT algorithm. The PD 2.4 processing workflow containing an additional node of Minora Feature Detector for precursor ion-based quantification was used for protein identification and protein relative quantitation analysis between samples. The database search was conducted against a *Mus musculus* database that contains 63,028 sequences downloaded from the National Center for Biotechnology Information. Two-missed trypsin cleavage sites were allowed. The peptide precursor tolerance was set to 10 parts per million (ppm), and fragment ion tolerance was set to 0.6 Da. Variable modification of methionine oxidation, deamidation of asparagines/glutamine, acetylation on protein N terminus, and fixed modification of cysteine carbamidomethylation were set for the database search. Only high-confidence peptides defined by Sequest HT with a 1% false discovery rate by Percolator were considered for the peptide identification. The final protein IDs contained protein groups that were filtered with at least two peptides per protein. Relative quantitation of identified proteins between the control and liraglutide-treated samples was determined by the label-free quantitation workflow in PD 2.4. The precursor abundance intensity for each peptide identified by MS/MS in each sample was automatically determined, and their unique razor peptides for each protein in each sample were summed and used for calculating the protein abundance by PD 2.4 software with normalization against the spike yeast enolase protein. Protein ratios were calculated on the basis of pairwise ratio for liraglutide treatment over control samples. Results were normalized and plotted as $\log_2$ fold change, and missing values were imputed as previously described (*78*). Multivariate analysis of the OPLS-DA was performed using MetaboAnalyst 5.0 software (*79*).

For targeted proteomics analysis of human islet–conditioned media samples presented in Fig. 6C, four targeted peptides [DSTLIMQLLR, TAFDEAIAELDTLSEESYK (2+), TAFDEAIAELDTLSEESYK (3+), and SVTEQGAELSNEER, with double or triple charges from protein 14-3-3-zeta] were selected for targeted protein quantification across all samples (fig. S5C). For targeted proteomics analysis of human islet–conditioned media samples presented in fig. S5D, two targeted peptides: GIVDQSQQAYQEAFEISK and SVTEQGAELSNEER, with double charges from protein 14-3-3-zeta were selected for targeted protein quantification across all samples (fig. S4F). For all targeted proteomics analyses, the FT-FT DDA raw files for HCD MS/MS were used for extracted-ion chromatograms (XICs) of the targeted masses by Xcalibur software with mass tolerance at 5 ppm for mass precision. After manual inspection, peptides with little or no interference were used for quantitation among the samples. A layout template file was then generated and applied to all LC-MS/MS raw data files yielding peak area of all peptides of interest. Relative quantitation of the protein 14-3-3-zeta between the control and liraglutide-treated samples was determined by comparing the peak area of the XICs for each of the targeted peptides. Protein ratios were then calculated on the basis of the average of each peptide pairwise ratio for liraglutide treatment over control samples.

Statistical methods

Data are presented as means ± SEM unless otherwise stated. In all studies, both male and female mice were included at equal numbers. The data did not differ between males and females and thus are presented together, apart from the in vivo IPGTT data from β cell GLP-1R WT mice with and without α cell ablation (Fig. 3 and fig. S3). All statistical analyses were performed using GraphPad Prism 8.00 for Mac. Data were analyzed by one-factor or two-factor analysis of variance (ANOVA) with Bonferroni's posttest or Student's *t* test, as indicated. Differences were considered significant at $P \leq 0.05$.

SUPPLEMENTARY MATERIALS

Supplementary material for this article is available at https://science.org/doi/10.1126/sciadv.abn3773

View/request a protocol for this paper from *Bio-protocol*.

REFERENCES AND NOTES

1. S. Mojsov, G. C. Weir, J. F. Habener, Insulinotropin: Glucagon-like peptide I (7-37) co-encoded in the glucagon gene is a potent stimulator of insulin release in the perfused rat pancreas. *J. Clin. Invest.* **79**, 616–619 (1987).
2. H. C. Fehmann, J. F. Habener, Insulinotropic hormone glucagon-like peptide-I(7-37) stimulation of proinsulin gene expression and proinsulin biosynthesis in insulinoma beta TC-1 cells. *Endocrinology* **130**, 159–166 (1992).
3. J. J. Meier, M. A. Nauck, D. Kranz, J. J. Holst, C. F. Deacon, D. Gaeckler, W. E. Schmidt, B. Gallwitz, Secretion, degradation, and elimination of glucagon-like peptide 1 and gastric inhibitory polypeptide in patients with chronic renal insufficiency and healthy control subjects. *Diabetes* **53**, 654–662 (2004).
4. L. Hansen, C. F. Deacon, C. Orskov, J. J. Holst, Glucagon-like peptide-1-(7-36)amide is transformed to glucagon-like peptide-1-(9-36)amide by dipeptidyl peptidase IV in the capillaries supplying the L cells of the porcine intestine. *Endocrinology* **140**, 5356–5363 (1999).
5. S. A. Campbell, D. P. Golec, M. Hubert, J. Johnson, N. Salamon, A. Barr, P. E. MacDonald, K. Philippaert, P. E. Light, Human islets contain a subpopulation of glucagon-like peptide-1 secreting α cells that is increased in type 2 diabetes. *Mol. Metab.* **39**, 101014 (2020).
6. R. Dusaulcy, S. Handgraaf, S. Skarupelova, F. Visentin, C. Vesin, M. Heddad-Masson, F. Reimann, F. Gribble, J. Philippe, Y. Gosmain, Functional and molecular adaptations of enteroendocrine L-cells in male obese mice are associated with preservation of pancreatic α-Cell function and prevention of hyperglycemia. *Endocrinology* **157**, 3832–3843 (2016).
7. G. Kilimnik, A. Kim, D. F. Steiner, T. C. Friedman, M. Hara, Intraislet production of GLP-1 by activation of prohormone convertase 1/3 in pancreatic α-cells in mouse models of β-cell regeneration. *Islets* **2**, 149–155 (2010).
8. P. Marchetti, R. Lupi, M. Bugliani, C. L. Kirkpatrick, G. Sebastiani, F. A. Grieco, S. Del Guerra, V. D'Aleo, S. Piro, L. Marselli, U. Boggi, F. Filipponi, L. Tinti, L. Salvini, C. B. Wollheim, F. Purrello, F. Dotta, A local glucagon-like peptide 1 (GLP-1) system in human pancreatic islets. *Diabetologia* **55**, 3262–3272 (2012).
9. K. Masur, E. C. Tibaduiza, C. Chen, B. Ligon, M. Beinborn, Basal receptor activation by locally produced glucagon-like peptide-1 contributes to maintaining beta-cell function. *Mol. Endocrinol.* **19**, 1373–1382 (2005).
10. R. C. Moffett, S. Vasu, B. Thorens, D. J. Drucker, P. R. Flatt, Incretin receptor null mice reveal key role of GLP-1 but not GIP in pancreatic beta cell adaptation to pregnancy. *PLOS ONE* **9**, e96863 (2014).
11. Y. Nie, M. Nakashima, P. L. Brubaker, Q. L. Li, R. Perfetti, E. Jansen, Y. Zambre, D. Pipeleers, T. C. Friedman, Regulation of pancreatic PC1 and PC2 associated with increased glucagon-like peptide 1 in diabetic rats. *J. Clin. Invest.* **105**, 955–965 (2000).
12. T. J. O'Malley, G. E. Fava, Y. Zhang, V. A. Fonseca, H. Wu, Progressive change of intra-islet GLP-1 production during diabetes development. *Diabetes Metab. Res. Rev.* **30**, 661–668 (2014).
13. N. M. Whalley, L. E. Pritchard, D. M. Smith, A. White, Processing of proglucagon to GLP-1 in pancreatic α-cells: Is this a paracrine mechanism enabling GLP-1 to act on β-cells? *J. Endocrinol.* **211**, 99–106 (2011).
14. Y. Song, J. A. Koehler, L. L. Baggio, A. C. Powers, D. A. Sandoval, D. J. Drucker, Gut-proglucagon-derived peptides are essential for regulating glucose homeostasis in mice. *Cell Metab.* **30**, 976–986.e3 (2019).
15. S. Kim, R. L. Whitener, H. Peiris, X. Gu, C. A. Chang, J. Y. Lam, J. Camunas-Soler, I. Park, R. J. Bevacqua, K. Tellez, S. R. Quake, J. R. T. Lakey, R. Bottino, P. J. Ross, S. K. Kim, Molecular and genetic regulation of pig pancreatic islet cell development. *Development* **147**, dev186213 (2020).
16. A. P. Chambers, J. E. Sorrell, A. Haller, K. Roelofs, C. R. Hutch, K.-S. Kim, R. Gutierrez-Aguilar, B. Li, D. J. Drucker, D. A. D'Alessio, R. J. Seeley, D. A. Sandoval, The role of pancreatic preproglucagon in glucose homeostasis in mice. *Cell Metab.* **25**, 927–934.e3 (2017).
17. K. S. Kim, C. R. Hutch, L. Wood, I. J. Magrisso, R. J. Seeley, D. A. Sandoval, Glycemic effect of pancreatic preproglucagon in mouse sleeve gastrectomy. *JCI Insight* **4**, e129452 (2019).
18. M. E. Capozzi, B. Svendsen, S. E. Encisco, S. L. Lewandowski, M. D. Martin, H. Lin, J. L. Jaffe, R. W. Coch, J. M. Haldeman, P. E. MacDonald, M. J. Merrins, D. A. D'Alessio, J. E. Campbell, β cell tone is defined by proglucagon peptides through cAMP signaling. *JCI Insight* **4**, e126742 (2019).
19. B. Svendsen, O. Larsen, M. B. N. Gabe, C. B. Christiansen, M. M. Rosenkilde, D. J. Drucker, J. J. Holst, Insulin secretion depends on intra-islet glucagon signaling. *Cell Rep.* **25**, 1127–1134.e2 (2018).
20. S. Traub, D. T. Meier, F. Schulze, E. Dror, T. M. Nordmann, N. Goetz, N. Koch, E. Dalmas, M. Stawiski, V. Makshana, F. Thorel, P. L. Herrera, M. Boni-Schnetzler, M. Y. Donath, Pancreatic α cell-derived glucagon-related peptides are required for β cell adaptation and glucose homeostasis. *Cell Rep.* **18**, 3192–3203 (2017).
21. M. Saikia, M. M. Holter, L. R. Donahue, I. S. Lee, Q. C. Zheng, J. L. Wise, J. E. Todero, D. J. Phuong, D. Garibay, R. Coch, K. W. Sloop, A. Garcia-Ocana, C. G. Danko, B. P. Cummings, GLP-1 receptor signaling increases PCSK1 and β cell features in human α cells. *JCI Insight* **6**, e141851 (2021).
22. D. Garibay, J. Lou, S. A. Lee, K. E. Zaborska, M. H. Weissman, E. Sloma, L. Donahue, A. D. Miller, A. C. White, M. D. Michael, K. W. Sloop, B. P. Cummings, β cell GLP-1R signaling alters α cell proglucagon processing after vertical sleeve gastrectomy in mice. *Cell Rep.* **23**, 967–973 (2018).
23. L. S. Jun, A. D. Showalter, N. Ali, F. Dai, W. Ma, T. Coskun, J. V. Ficorilli, M. B. Wheeler, M. D. Michael, K. W. Sloop, A novel humanized GLP-1 receptor model enables both affinity purification and Cre-LoxP deletion of the receptor. *PLOS ONE* **9**, e93746 (2014).
24. B. Wicksteed, M. Brissova, W. Yan, D. M. Opland, J. L. Plank, R. B. Reinert, L. M. Dickson, N. A. Tamarina, L. H. Philipson, A. Shostak, E. Bernal-Mizrachi, L. Elghazi, M. W. Roe, P. A. Labosky, M. G. Myers Jr., M. Gannon, A. C. Powers, P. J. Dempsey, Conditional gene targeting in mouse pancreatic β-cells: Analysis of ectopic Cre transgene expression in the brain. *Diabetes* **59**, 3090–3098 (2010).
25. F. Thorel, N. Damond, S. Chera, A. Wiederkehr, B. Thorens, P. Meda, C. B. Wollheim, P. L. Herrera, Normal glucagon signaling and β-cell function after near-total α-cell ablation in adult mice. *Diabetes* **60**, 2872–2882 (2011).
26. C. Kapitza, M. Zdravkovic, C. Hindsberger, A. Flint, The effect of the once-daily human glucagon-like peptide 1 analog liraglutide on the pharmacokinetics of acetaminophen. *Adv. Ther.* **28**, 650–660 (2011).
27. M. Horowitz, A. Flint, K. L. Jones, C. Hindsberger, M. F. Rasmussen, C. Kapitza, S. Doran, T. Jax, M. Zdravkovic, I. M. Chapman, Effect of the once-daily human GLP-1 analogue liraglutide on appetite, energy intake, energy expenditure and gastric emptying in type 2 diabetes. *Diabetes Res. Clin. Pract.* **97**, 258–266 (2012).
28. D. Flamez, P. Gilon, K. Moens, A. Van Breusegem, D. Delmeire, L. A. Scrocchi, J. C. Henquin, D. J. Drucker, F. Schuit, Altered cAMP and Ca^{2+} signaling in mouse pancreatic islets with glucagon-like peptide-1 receptor null phenotype. *Diabetes* **48**, 1979–1986 (1999).
29. E. P. Smith, Z. An, C. Wagner, A. G. Lewis, E. B. Cohen, B. Li, P. Mahbod, D. Sandoval, D. Perez-Tilve, N. Tamarina, L. H. Philipson, D. A. Stoffers, R. J. Seeley, D. A. D'Alessio, The role of β cell glucagon-like peptide-1 signaling in glucose regulation and response to diabetes drugs. *Cell Metab.* **19**, 1050–1057 (2014).
30. S. Merani, W. Truong, J. A. Emamaullee, C. Toso, L. B. Knudsen, A. M. J. Shapiro, Liraglutide, a long-acting human glucagon-like peptide 1 analog, improves glucose homeostasis in marginal mass islet transplantation in mice. *Endocrinology* **149**, 4322–4328 (2008).
31. B. Wu, S. Wei, N. Petersen, Y. Ali, X. Wang, T. Bacaj, P. Rorsman, W. Hong, T. C. Südhof, W. Han, Synaptotagmin-7 phosphorylation mediates GLP-1–dependent potentiation of insulin secretion from β-cells. *Proc. Natl. Acad. Sci. U.S.A.* **112**, 9996–10001 (2015).
32. D. Garibay, A. K. McGavigan, S. A. Lee, J. V. Ficorilli, A. L. Cox, M. D. Michael, K. W. Sloop, B. P. Cummings, β-cell glucagon-like peptide-1 receptor contributes to improved glucose tolerance after vertical sleeve gastrectomy. *Endocrinology* **157**, 3405–3409 (2016).
33. S. Jia, A. Ivanov, D. Blasevic, T. Müller, B. Purfürst, W. Sun, W. Chen, M. N. Poy, N. Rajewsky, C. Birchmeier, Insm1 cooperates with Neurod1 and Foxa2 to maintain mature pancreatic β-cell function. *EMBO J.* **34**, 1417–1433 (2015).
34. J. J. A. Armenteros, K. D. Tsirigos, C. K. Sønderby, T. N. Petersen, O. Winther, S. Brunak, G. von Heijne, H. Nielsen, SignalP 5.0 improves signal peptide predictions using deep neural networks. *Nat. Biotechnol.* **37**, 420–423 (2019).
35. G. E. Lim, M. Piske, J. E. Lulo, H. S. Ramshaw, A. F. Lopez, J. D. Johnson, Ywhaz/14-3-3ζ deletion improves glucose tolerance through a GLP-1-dependent mechanism. *Endocrinology* **157**, 2649–2659 (2016).
36. C. Petosa, S. C. Masters, L. A. Bankston, J. Pohl, B. Wang, H. Fu, R. C. Liddington, 14-3-3zeta binds a phosphorylated Raf peptide and an unphosphorylated peptide via its conserved amphipathic groove. *J. Biol. Chem.* **273**, 16305–16310 (1998).
37. Y. Mugabo, C. Zhao, J. J. Tan, A. Ghosh, S. A. Campbell, E. Fadzeyeva, F. Paré, S. S. Pan, M. Galipeau, J. Ast, J. Broichhagen, D. J. Hodson, E. E. Mulvihill, S. Petropoulos, G. E. Lim, 14-3-3ζ constrains insulin secretion by regulating mitochondrial function in pancreatic β-cells. *JCI Insight* **7**, e156378 (2022).
38. L. Zhu, D. Dattaroy, J. Pham, L. Wang, L. F. Barella, Y. Cui, K. J. Wilkins, B. L. Roth, U. Hochgeschwender, F. M. Matschinsky, K. H. Kaestner, N. M. Doliba, J. Wess, Intra-islet glucagon signaling is critical for maintaining glucose homeostasis. *JCI Insight* **5**, e127994 (2019).
39. S. Ueno, Y. Seino, S. Hidaka, R. Maekawa, Y. Takano, M. Yamamoto, M. Hori, K. Yokota, A. Masuda, T. Himeno, S. Tsunekawa, H. Kamiya, J. Nakamura, H. Kuwata, H. Fujisawa, M. Shibata, T. Takayanagi, Y. Sugimura, D. Yabe, Y. Hayashi, A. Suzuki, High protein diet

feeding aggravates hyperaminoacidemia in mice deficient in proglucagon-derived peptides. *Nutrients* **14**, 975 (2022).
40. M. Winther-Sørensen, K. D. Galsgaard, A. Santos, S. A. J. Trammell, K. Sulek, R. E. Kuhre, J. Pedersen, D. B. Andersen, A. S. Hassing, M. Dall, J. T. Treebak, M. P. Gillum, S. S. Torekov, J. A. Windeløv, J. E. Hunt, S. A. S. Kjeldsen, S. L. Jepsen, C. G. Vasilopoulou, F. K. Knop, C. Ørskov, M. P. Werge, H. C. Bisgaard, P. L. Eriksen, H. Vilstrup, L. L. Gluud, J. J. Holst, N. J. W. Albrechtsen, Glucagon acutely regulates hepatic amino acid catabolism and the effect may be disturbed by steatosis. *Mol. Metab.* **42**, 101080 (2020).
41. C. Watanabe, Y. Seino, H. Miyahira, M. Yamamoto, A. Fukami, N. Ozaki, Y. Takagishi, J. Sato, T. Fukuwatari, K. Shibata, Y. Oiso, Y. Murata, Y. Hayashi, Remodeling of hepatic metabolism and hyperaminoacidemia in mice deficient in proglucagon-derived peptides. *Diabetes* **61**, 74–84 (2012).
42. E. Durden, G. Lenhart, L. Lopez-Gonzalez, M. Hammer, J. Langer, Predictors of glycemic control and diabetes-related costs among type 2 diabetes patients initiating therapy with liraglutide in the United States. *J. Med. Econ.* **19**, 403–413 (2016).
43. G. B. Flock, X. Cao, M. Maziarz, D. J. Drucker, Activation of enteroendocrine membrane progesterone receptors promotes incretin secretion and improves glucose tolerance in mice. *Diabetes* **62**, 283–290 (2013).
44. S. Handgraaf, R. Dusaulcy, F. Visentin, J. Philippe, Y. Gosmain, 17-β estradiol regulates proglucagon-derived peptide secretion in mouse and human α- and L cells. *JCI Insight* **3**, e98569 (2018).
45. S. Matsumoto, M. Yamazaki, M. Kadono, H. Iwase, K. Kobayashi, H. Okada, M. Fukui, G. Hasegawa, N. Nakamura, Effects of liraglutide on postprandial insulin and glucagon responses in Japanese patients with type 2 diabetes. *J. Clin. Biochem. Nutr.* **53**, 68–72 (2013).
46. K. Moens, D. Flamez, C. Van Schravendijk, Z. Ling, D. Pipeleers, F. Schuit, Dual glucagon recognition by pancreatic beta-cells via glucagon and glucagon-like peptide 1 receptors. *Diabetes* **47**, 66–72 (1998).
47. E. Muscelli, A. Mari, A. Casolaro, S. Camastra, G. Seghieri, A. Gastaldelli, J. J. Holst, E. Ferrannini, Separate impact of obesity and glucose tolerance on the incretin effect in normal subjects and type 2 diabetic patients. *Diabetes* **57**, 1340–1348 (2008).
48. E. Rask, T. Olsson, S. Söderberg, O. Johnson, J. Seckl, J. J. Holst, B. Ahrén; Northern Sweden Monitoring of Trends and Determinants in Cardiovascular Disease (MONICA), Impaired incretin response after a mixed meal is associated with insulin resistance in nondiabetic men. *Diabetes Care* **24**, 1640–1645 (2001).
49. P. Richards, R. Pais, A. M. Habib, C. A. Brighton, G. S. H. Yeo, F. Reimann, F. M. Gribble, High fat diet impairs the function of glucagon-like peptide-1 producing L-cells. *Peptides* **77**, 21–27 (2016).
50. M. B. Toft-Nielsen, M. B. Damholt, S. Madsbad, L. M. Hilsted, T. E. Hughes, B. K. Michelsen, J. J. Holst, Determinants of the impaired secretion of glucagon-like peptide-1 in type 2 diabetic patients. *J. Clin. Endocrinol. Metab.* **86**, 3717–3723 (2001).
51. T. Vilsboll, T. Krarup, C. F. Deacon, S. Madsbad, J. J. Holst, Reduced postprandial concentrations of intact biologically active glucagon-like peptide 1 in type 2 diabetic patients. *Diabetes* **50**, 609–613 (2001).
52. M. B. Yaffe, K. Rittinger, S. Volinia, P. R. Caron, A. Aitken, H. Leffers, S. J. Gamblin, S. J. Smerdon, L. C. Cantley, The structural basis for 14-3-3: Phosphopeptide binding specificity. *Cell* **91**, 961–971 (1997).
53. E. F. Barry, F. A. Felquer, J. A. Powell, L. Biggs, F. C. Stomski, A. Urbani, H. Ramshaw, P. Hoffmann, M. C. Wilce, M. A. Grimbaldeston, A. F. Lopez, M. A. Guthridge, 14-3-3: Shc scaffolds integrate phosphoserine and phosphotyrosine signaling to regulate phosphatidylinositol 3-kinase activation and cell survival. *J. Biol. Chem.* **284**, 12080–12090 (2009).
54. D. Roth, R. D. Burgoyne, Stimulation of catecholamine secretion from adrenal chromaffin cells by 14-3-3 proteins is due to reorganisation of the cortical actin network. *FEBS Lett.* **374**, 77–81 (1995).
55. A. Brunet, F. Kanai, J. Stehn, J. Xu, D. Sarbassova, J. V. Frangioni, S. N. Dalal, J. A. DeCaprio, M. E. Greenberg, M. B. Yaffe, 14-3-3 transits to the nucleus and participates in dynamic nucleocytoplasmic transport. *J. Cell Biol.* **156**, 817–828 (2002).
56. S. Chen, S. Synowsky, M. Tinti, C. MacKintosh, The capture of phosphoproteins by 14-3-3 proteins mediates actions of insulin. *Trends Endocrinol. Metab.* **22**, 429–436 (2011).
57. S. S. Neukamm, J. Ott, S. Dammeier, R. Lehmann, H. U. Häring, E. Schleicher, C. Weigert, Phosphorylation of serine 1137/1138 of mouse insulin receptor substrate (IRS) 2 regulates cAMP-dependent binding to 14-3-3 proteins and IRS2 protein degradation. *J. Biol. Chem.* **288**, 16403–16415 (2013).
58. G. E. Lim, M. Piske, J. D. Johnson, 14-3-3 proteins are essential signalling hubs for beta cell survival. *Diabetologia* **56**, 825–837 (2013).
59. S. G. Tattikota, M. D. Sury, T. Rathjen, H. H. Wessels, A. K. Pandey, X. You, C. Becker, W. Chen, M. Selbach, M. N. Poy, Argonaute2 regulates the pancreatic β-cell secretome. *Mol. Cell. Proteomics* **12**, 1214–1225 (2013).
60. G. E. Lim, T. Albrecht, M. Piske, K. Sarai, J. T. C. Lee, H. S. Ramshaw, S. Sinha, M. A. Guthridge, A. Acker-Palmer, A. F. Lopez, S. M. Clee, C. Nislow, J. D. Johnson, 14-3-3ζ coordinates adipogenesis of visceral fat. *Nat. Commun.* **6**, 7671 (2015).
61. C. Talchai, S. Xuan, H. V. Lin, L. Sussel, D. Accili, Pancreatic β cell dedifferentiation as a mechanism of diabetic β cell failure. *Cell* **150**, 1223–1234 (2012).
62. S. Tsunekawa, N. Yamamoto, K. Tsukamoto, Y. Itoh, Y. Kaneko, T. Kimura, Y. Ariyoshi, Y. Miura, Y. Oiso, I. Niki, Protection of pancreatic Beta-cells by exendin-4 may involve the reduction of endoplasmic reticulum stress; in vivo and in vitro studies. *J. Endocrinol.* **193**, 65–74 (2007).
63. M. Shimoda, Y. Kanda, S. Hamamoto, K. Tawaramoto, M. Hashiramoto, M. Matsuki, K. Kaku, The human glucagon-like peptide-1 analogue liraglutide preserves pancreatic beta cells via regulation of cell kinetics and suppression of oxidative and endoplasmic reticulum stress in a mouse model of diabetes. *Diabetologia* **54**, 1098–1108 (2011).
64. C. Dai, Y. Hang, A. Shostak, G. Poffenberger, N. Hart, N. Prasad, N. Phillips, S. E. Levy, D. L. Greiner, L. D. Shultz, R. Bottino, S. K. Kim, A. C. Powers, Age-dependent human β cell proliferation induced by glucagon-like peptide 1 and calcineurin signaling. *J. Clin. Investig.* **127**, 3835–3844 (2017).
65. L. Ahlkvist, K. Brown, B. Ahrén, Upregulated insulin secretion in insulin-resistant mice: Evidence of increased islet GLP1 receptor levels and GPR119-activated GLP1 secretion. *Endocr. Connect.* **2**, 69–78 (2013).
66. S. A. Herzberg-Schäfer, H. Staiger, M. Heni, C. Ketterer, M. Guthoff, K. Kantartzis, F. Machicao, N. Stefan, H.-U. Häring, A. Fritsche, Evaluation of fasting state–/oral glucose tolerance test-derived measures of insulin release for the detection of genetically impaired β-cell function. *PLOS ONE* **5**, e14194 (2010).
67. L. Liu, Y. Huang, C. Fang, H. Zhang, J. Yang, C. Xuan, F. Wang, H. Lu, S. Cao, Y. Wang, S. Li, J. Sha, M. Zha, M. Guo, J. Wang, Chronic noise-exposure exacerbates insulin resistance and promotes the manifestations of the type 2 diabetes in a high-fat diet mouse model. *PLOS ONE* **13**, e0195411 (2018).
68. G. Pacini, B. Omar, B. Ahrén, Methods and models for metabolic assessment in mice. *J. Diabetes Res.* **2013**, 986906 (2013).
69. V. A. Salunkhe, I. G. Mollet, J. K. Ofori, H. A. Malm, J. L. S. Esguerra, T. M. Reinbothe, K. G. Stenkula, A. Wendt, L. Eliasson, J. Vikman, Dual effect of rosuvastatin on glucose homeostasis through improved insulin sensitivity and reduced insulin secretion. *EBioMedicine* **10**, 185–194 (2016).
70. L. Zhang, J. Chen, H. Fu, Suppression of apoptosis signal-regulating kinase 1-induced cell death by 14-3-3 proteins. *Proc. Natl. Acad. Sci. U.S.A.* **96**, 8511–8515 (1999).
71. Y. Du, S. C. Masters, F. R. Khuri, H. Fu, Monitoring 14-3-3 protein interactions with a homogeneous fluorescence polarization assay. *J. Biomol. Screen.* **11**, 269–276 (2006).
72. B. Wang, H. Yang, Y. C. Liu, T. Jelinek, L. Zhang, E. Ruoslahti, H. Fu, Isolation of high-affinity peptide antagonists of 14-3-3 proteins by phage display. *Biochemistry* **38**, 12499–12504 (1999).
73. M. D. Escobar, J. L. Hunt, A cost-effective RNA extraction technique from animal cells and tissue using silica columns. *J. Biol. Methods* **4**, e72 (2017).
74. G. E. Lim, G. J. Huang, N. Flora, D. LeRoith, C. J. Rhodes, P. L. Brubaker, Insulin regulates glucagon-like peptide-1 secretion from the enteroendocrine L cell. *Endocrinology* **150**, 580–591 (2009).
75. Y. Yang, E. Anderson, S. Zhang, Evaluation of six sample preparation procedures for qualitative and quantitative proteomics analysis of milk fat globule membrane. *Electrophoresis* **39**, 2332–2339 (2018).
76. A. Zougman, P. J. Selby, R. E. Banks, Suspension trapping (STrap) sample preparation method for bottom-up proteomics analysis. *Proteomics* **14**, 1006–1000 (2014).
77. R. M. Harman, M. K. He, S. Zhang, G. R. van de Walle, Plasminogen activator inhibitor-1 and tenascin-C secreted by equine mesenchymal stromal cells stimulate dermal fibroblast migration in vitro and contribute to wound healing in vivo. *Cytotherapy* **20**, 1061–1076 (2018).
78. J. T. Aguilan, K. Kulej, S. Sidoli, Guide for protein fold change and p-value calculation for non-experts in proteomics. *Mol. Omics* **16**, 573–582 (2020).
79. E. A. Thévenot, A. Roux, Y. Xu, E. Ezan, C. Junot, Analysis of the human adult urinary metabolome variations with age, body mass index, and gender by implementing a comprehensive workflow for univariate and OPLS statistical analyses. *J. Proteome Res.* **14**, 3322–3335 (2015).

Acknowledgments: We thank the Proteomics and Metabolomics Facility of Cornell University for providing the mass spectrometry data and NIH SIG 1S10 OD017992-01 grant support for the Orbitrap Fusion mass spectrometer. We would like to thank J. Belliveau for assistance with animal care and G. Van de Walle for helpful input on the conditioned media studies. We thank P. Herrera for generating the original the *GcgDTR* mouse model and approving our access to it. We are grateful to the Integrated Islet Distribution Program (supported by NIH 2UC4DK098085) for the provision of human islets through their Islet Award Initiative supported through JDRF. Illustrations created on BioRender.com. **Funding:** This work was

supported by the Department of Defense (W81XWH-18-1-0206), the Hartwell Foundation, and the NIH/NIDDK (R56DK124853 and F30DK126538). **Author contributions:** M.M.H. contributed to study design, collected and analyzed data, and wrote the manuscript. D.J.P., I.L., S.F., L.W., E.T.A., and Q.F. collected and/or analyzed data and revised the manuscript. M.S., S.Z., and K.W.S. contributed to study design and data interpretation and revised the manuscript. B.P.C. supervised the study, contributed to study design and data analysis, and finalized the manuscript. **Competing interests:** The authors declare that they have no competing interests, except that K.W.S. is employed by Eli Lilly and Company and owns Eli Lilly and Company stock.

Data and materials availability: All data needed to evaluate the conclusions in the paper are present in the paper and/or the Supplementary Materials. Contact K.W.S. for a material transfer agreement to obtain the floxed GLP-1R mouse line.

Submitted 30 November 2021
Accepted 8 June 2022
Published 22 July 2022
10.1126/sciadv.abn3773